ADVANCED MATERIALS
www.advmat.de

Rubbery Electronics Fully Made of Stretchable Elastomeric Electronic Materials

*Kyoseung Sim, Zhoulyu Rao, Faheem Ershad, and Cunjiang Yu**

Stretchable electronics outperform existing rigid and bulky electronics and benefit a wide range of species, including humans, machines, and robots, whose activities are associated with large mechanical deformation and strain. Due to the nonstretchable nature of most electronic materials, in particular semiconductors, stretchable electronics are mostly realized through the strategies of architectural engineering to accommodate mechanical stretching rather than imposing strain into the materials directly. On the other hand, recent development of stretchable electronics by creating them entirely from stretchable elastomeric electronic materials, i.e., rubbery electronics, suggests a feasible a venue. Rubbery electronics have gained increasing interest due to the unique advantages that they and their associated manufacturing technologies have offered. This work reviews the recent progress in developing rubbery electronics, including the crucial stretchable elastomeric materials of rubbery conductors, rubbery semiconductors, and rubbery dielectrics. Thereafter, various rubbery electronics such as rubbery transistors, integrated electronics, rubbery optoelectronic devices, and rubbery sensors are discussed.

1. Introduction

In the past few decades, the development of wafer electronics, primarily in rigid and bulky formats, has led to a significantly improved quality of life, standard of living, healthcare, security, etc. Recent fast advances in electronic materials, fabrication processes, and device structures have been transforming traditional wafer electronics to be soft, stretchy, and reconfigurable. In particular, owing to their superior mechanical characteristics, i.e., soft, bendable, stretchable, and twistable, stretchable electronics hold promise in health monitors,[1] medical implants,[2–10] artificial skins,[5,6,11–15] human–machine interfaces,[11,16–20] wearable internet of things,[21–24] etc.

As the core and fundamental building block of active electronics, transistors constructed from semiconductors, conductors, and dielectrics are key to enabling electrical functionalities such as switching and amplification. To make transistors stretchable, either the associated electronic materials need to be stretchable or special mechanical structures and layouts need to be included in the transistor design. There are many studies reporting stretchable conductors, as reviewed in the following, while many readily available dielectric materials are stretchy. These have significantly offered many possible options in the device design space. To date, the dominant semiconductors employed for stretchable electronics are either conventional or emerging semiconductors. However, these materials, either in the format of inorganics (such as Si, GaAs, oxides) or organics (such as poly(3-hexylthiophene-2,5-diyl) or P3HT, pentacene), are mechanically nonstretchable.[20,21] Existing strategies to make these nonstretchable semiconductors stretchable mainly involve creating special mechanical structures or architectures with these materials, such as out-of-plane wrinkles,[25,26] in-plane serpentines,[27,28] rigid islands with deformable interconnects,[29–31] and kirigami architectures,[32–34] to eliminate mechanical strain while they are stretched. However, these approaches require sophisticated structural designs, complicated manufacturing processes, or consume a large area due to stretchable interconnection, all of which pose substantial challenges in high-density integration, packaging, associated high cost, and mass production.

Constructing devices all from intrinsically stretchable elastomeric electronic materials offers another interesting yet promising route toward stretchable transistors and electronics. These types of electronics, namely rubbery electronics, neatly avoid the aforementioned challenges since they do not require structural engineering for device fabrication and the manufacturing processes can be adopted into conventional fabrication processes.[29,35] In addition, rubbery electronics offer better cost

Dr. K. Sim, Prof. C. Yu
Department of Mechanical Engineering
University of Houston
Houston, TX 77204, USA
E-mail: cyu15@uh.edu
Z. Rao, Prof. C. Yu
Materials Science and Engineering Program
University of Houston
Houston, TX 77204, USA
F. Ershad, Prof. C. Yu
Department of Biomedical Engineering
University of Houston
Houston, TX 77204, USA
Prof. C. Yu
Department of Electrical and Computer Engineering
Texas Center for Superconductivity
University of Houston
Houston, TX 77204, USA
The ORCID identification number(s) for the author(s) of this article can be found under https://doi.org/10.1002/adma.201902417.

DOI: 10.1002/adma.201902417

effectiveness, higher mechanical durability, larger strain tolerance, and tunability.[31–34,36] In the development of rubbery electronics, the elastomeric semiconductor is a core material. Very recently, there has been some progress in developing intrinsically stretchable rubbery semiconductors and their stretchable electronics.[37–69]

Here, we present recent progress in rubbery electronics with four categorized sections, in the following order: 1) rubbery conductors, 2) rubbery semiconductors, 3) rubbery dielectrics, and 4) rubbery electronics. Each section overviews the importance and background of the respective rubbery electronic components or devices, and then introduces representative studies with detailed reviews. Finally, we conclude the review with a discussion on the challenges and opportunities in rubbery electronics.

2. Rubbery Conductors

Rubbery conductors are essential components for rubbery electronics such as transistors, integrated electronics, etc.[64,70] Conductors that are intrinsically stretchable with mechanical stretchability (>20%) generally exist in two formats. One is stretchable conductive polymers and the other is nanocomposites of nanoconductor fillers in insulating rubber matrices. Some conductive polymers through rationalized chemical treatments are capable of not only achieving an excellent electrical conductivity of 4100 S cm^{-1}, but also a mechanical stretchability of 100%.[71] Inheriting the mechanical stretchability of rubbers, nanomaterials such as 0D nanoparticles (NPs), 1D nanowires/nanotubes (NWs/NTs), and 2D nanosheets (NSs) based rubbery composites have both properties of stretchability and electrical conductivity. These rubbery nanocomposites can achieve the conductivity of metal[72] and a stretchability up to 700%. Rubbery conductors have been briefly organized into two types: stretchable conductive polymers and nanomaterial based rubbery composites.

2.1. Stretchable Conductive Polymers

Due to their highly conjugated backbones that are in oxidized or reduced states, conductive polymers are electrically conductive.[73–75] In addition, because of the merits such as low moduli, chemistry-structure-properties tunability, and easy and scalable processing, conductive polymers have been investigated for many unique electronic and optoelectronic applications.[75–80] By doping conductive polymers with bulky organic anions, they can be easily processed in solution formats used in conventional processing techniques, such as spin-coating[81] and printing.[82] There are now many available conductive polymers including polyacetylene, polypyrrole (PPy), polyaniline (PANi), polythiophene, and their derivatives (**Figure 1**a).[83–85] Among them, poly(3,4-ethylenedioxythiophene) polystyrene sulfonate (PEDOT:PSS) is the most intensively investigated conductive electrode material owing to its excellent electrical conductivity,[86] transparency,[87] chemical stability,[88] biocompatibility,[89] solution processability,[90] and commercial availability. PEDOT:PSS films derived from commercially available aqueous dispersions have a low conductivity normally around 1 S cm^{-1}[86,91,92] with a fracture limit around 6%,[70,93] which indicates that the films are not stretchable or are not able to

Kyoseung Sim received his Ph.D. degree from materials science and engineering from the University of Houston in 2018. He is currently a post-doctoral research fellow in Mechanical Engineering in University of Houston. He was a researcher in Daegu Gyeongbuk Institute of Science and Technology (South Korea) from 2010 to 2013, where he was involved in research on photovoltaics. From 2013 to 2014, he was involved in research on organic single molecule-based field effect transistors with the Center for Electro-Photo Behaviors in Advanced Molecular Systems, Pohang University of Science and Technology (South Korea). His current research interests are wearable and implantable soft electronics.

Zhoulyu Rao received his B.S. degree in applied chemistry from Xidian University, Xi'an, Shaanxi, China, in 2012, and M.S. in chemistry from the University of Science and Technology of China, Hefei, Anhui, China, in 2015. He is currently pursuing his Ph.D. degree in material science engineering from the University of Houston, Houston, Texas, USA. His current research interest and focus is on device microfabrication and soft, wearable, and implantable electronics.

Cunjiang Yu received his Ph.D. degree in mechanical engineering from Arizona State University in 2010. He was trained as a post-doctoral fellow in the Department of Materials Science and Engineering, at the University of Illinois at Urbana-Champaign before joining the University of Houston in 2013. He is currently the Bill D. Cook Assistant Professor with the Department of Mechanical Engineering, University of Houston. He holds joint appointments in the Departments of Electrical and Computer Engineering, Biomedical Engineering, Materials Science and Engineering Program, and the Texas Center for Superconductivity. His current research interests include soft electronics, biointegrated electronics.

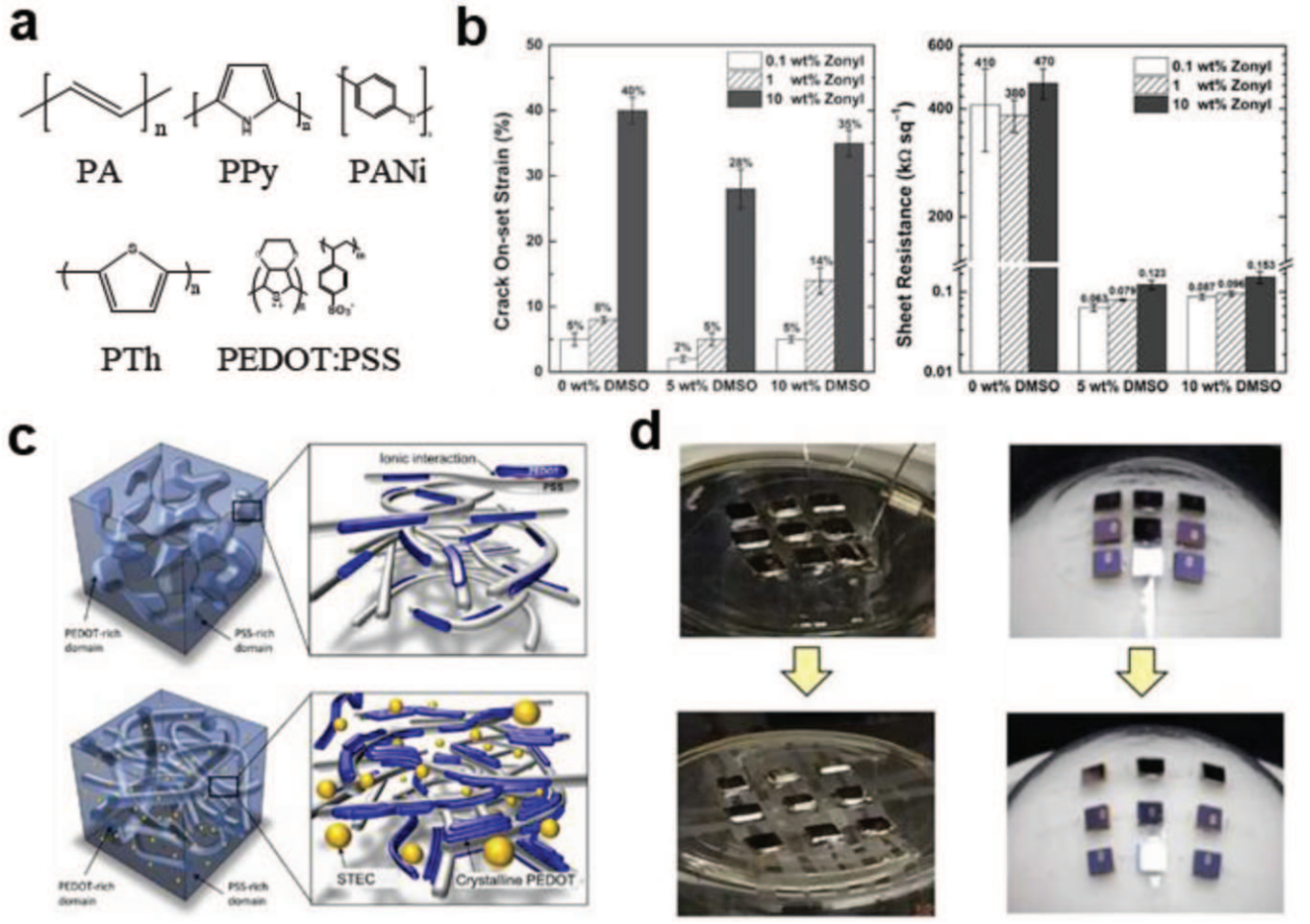

Figure 1. Stretchable conductive polymers. a) Chemical structures of some conductive polymers. b) Crack on-set strain (left) and sheet resistance (right) of PEDOT:PSS with different concentrations of DMSO and Zonyl. Reproduced with permission.[80] Copyright 2014, Wiley-VCH. c) Schematic illustration of the morphology of a typical PEDOT:PSS film (top) and a superior conductive stretchable PEDOT film with enhancers (bottom). d) High-density stretchable FET array being stretched on a flat surface and a spherical object, respectively. Reproduced under the terms and conditions of the CC-BY-NC 4.0 Creative Commons Attribution NonCommercial License 4.0.[71] Copyright 2017, The Authors, published by the American Association for the Advancement of Science.

meet the requirements of a typical stretchable conductor with stretchability greater than tens of percents.

However, their stretchability and conductivity can be improved either by secondary doping or post-treatment. Secondary dopants such as polar solvents,[94] surfactants,[76,80,95] ion liquid,[70,92] and other additives improve the conductivity of PEDOT:PSS by either additional doping effects or screening effects.[91] Another approach to improve the conductivity is to treat PEDOT:PSS films with solvents like methane and dimethyl sulfoxide (DMSO), or acids, like concentrated H_2SO_4.[86,93] Additives like Zonyl, Triton X-100, and ion liquid also improve the stretchability of PEDOT:PSS films,[76,80,92] while polar solvents[94] make PEDOT:PSS films more brittle with decreased fracture limits. Suchol et al. investigated the impact of DMSO and Zonyl on the mechanical and electrical properties of spin-coated PEDOT:PSS films (Figure 1b).[80] With only 1 wt% Zonyl, the tensile modulus of the PEDOT:PSS film dramatically decreased by a factor of eight. By optimizing the concentration of Zonyl and DMSO, 35% stretchability and a sheet resistance of 153 Ω sq^{-1} were achieved. Yue et al. reported a superior PEDOT:PSS film by adding ionic additives and other enhancers as conductivity-enhancing dopants into the PEDOT:PSS aqueous dispersion (Figure 1c).[70] Interestingly, from 0% to 100% strain, the conductivity of the PEDOT:PSS film increased from 3100 to 4100 S cm^{-1} because the PEDOT chain alignment along the direction of stretching improved. The PEDOT:PSS film was highly durable under cyclic loading, with the conductivity maintained at 3600 S cm^{-1} even after 1000 cycles from 0% to 100% strain. Based on this highly stretchable PEDOT:PSS, a high density field effect transistor (FET) array was demonstrated (Figure 1d).

2.2. Nanomaterials based Rubber Composites

Most rubbery conductors have been achieved through composite engineering of rubbers with percolated conductive nanomaterial fillers (e.g., 0D NPs,[96,97] 1D NWs and NTs, and 2D NSs).[98,99] The mechanical and electrical properties of

the rubbery composites can be tuned by altering the rubbery matrices, form factors of the conductive fillers, filling density, and degree of dispersion.[100–102] To incorporate conductive fillers into rubbers, there are several strategies including filtrating rubber into conductive filler networks,[103] synthesizing metallic fillers within rubbers,[97] mixing conductive fillers with rubbers,[104] and injecting fillers into rubbers.[72]

Based on the percolation theory, the percolation threshold of the rubbery conductive composites depends on the different form factors of the nanomaterial fillers[105,106]

$$V_{c\_0D} = \frac{\pi D^3}{6(D + D_{IP})^3} \tag{1}$$

$$V_{c\_1D} = \frac{5.71}{L^2} \tag{2}$$

$$V_{c\_2D} = \frac{27\pi D^2 t}{4(D + D_{IP})^3} \tag{3}$$

where V_c is the percolation threshold volume fraction of nanomaterials and D_{IP} is the interparticle distance. D is the particle diameter of 0D NPs or lateral diameter of 2D NSs, t is the thickness of 2D NSs, and L is the length of 1D NWs and NTs. Furthermore, the following expression defines the conductivity of the percolation network (σ) based on filler density

$$\sigma \propto (N - N_c)^t \tag{4}$$

where N is the density of the conducting fillers and t is the critical exponent of the conductivity, normally ranging from 1.0 to 10.[107,108] Interparticle contact resistance dominates the total resistance whereas the resistance of highly conductive metallic filler contributes negligibly.[109] When D_{IP} is equal to or less than the tunneling cut-off distance, typically 10 nm, electrons tend to hop over the NP-NP gap according to the quantum tunneling mechanism, which results in a current transport path inside the rubber. This leads to a rapid improvement in electrical conductivity of the percolated nanomaterials.

Due to their low aspect ratio, the NPs' percolation threshold (V_c) is 10 to 100 times higher than that of NWs.[110] Moreover, a large number of NP-NP junctions leads to high contact resistance and scattering of charge carriers. However, a rubbery matrix provides greater freedom for NPs because it enables reversible nanoscale restructuring and reconfiguration. Yoonseob et al. developed an AuNPs based stretchable conductive rubber (polyurethane, PU) fabricated by a vacuum-assisted filtration assembly.[110] AuNPs in PU formed chains of 10–40 NPs during fabrication, offering transport paths for electrons. When stretched, the NPs initially became disorganized, but as the strain increased, they gradually self-organized into bands along the stretching direction, which allowed the composite to retain its high electrical conductivity, shown in **Figure 2**a. This self-assembly behavior was reversible and reconfigurable after five consecutive cycles. Five layers of the rubbery conductor made by this method had a conductivity of 1800 S cm^{-1} at 0% strain, 210 S cm^{-1} at 60% strain, and 94 S cm^{-1} at 110% strain.

Liquid metals and their low-melting point alloys that are in liquid phase near room temperature are another form of a 0D nanomaterial. Gallium-based liquid metals such as EGaIn (75% gallium and 25% indium) and Galinstan (68.5% gallium, 21.5% indium, and 10% tin) are the most commonly investigated as conductive fillers due to their low toxicity, high electrical conductivity, negligible vapor pressure, and intrinsic deformability, and stretchability. The presence of liquid metal in rubbers has little harm on the mechanical properties of the host rubbers. Liquid metals are incorporated by filling the microchannels in rubbers to form rubbery conductors. Ha et al. demonstrated a stretchable acoustic device (SAD) by injecting Galinstan into a micropatterned elastomer channel, shown in Figure 2b.[72] The liquid metal coil had excellent electrical conductivity (3.46×10^6 S m^{-1} at 20 °C) at the initial state and can be stretched uniaxially up to 50% and biaxially up to 30% with only a 6% increase in resistance. Simultaneously, the SAD maintained its performance without any noticeable deviation from 1 to 20 kHz under the same stretched conditions. Michael et al. innovated more stretchable fibers with EGaIn fillers in the core of the hollow poly [styreneb-(ethylene-co-butylene)-b-styrene] (SEBS) resin fibers (Figure 2c).[111] The injected liquid metal had little impact on the mechanical and tactile properties of the fibers. The fibers were highly conductive as metallic wires and sustained their conductivity even at 700% strain through optimizing their size. Liquid metal droplets can also be dispersed into rubbers by ultrasonication, shear-mixing, acoustic wavers, and microfluidic flow focusing.

Conductive fillers are not limited to just 0D materials, however. Longer NWs and other 1D materials reduce required wire–wire contacts inducing higher conductivity at a given conductive filler density: this is essential for stretchability. When strain is applied, cracks or defects tend to appear at the boundary areas, which experience increased interparticle distance, resulting in a large sacrifice in conductivity. AgNWs have received extensive attention due to their high conductivity and good mechanical durability among all metallic nanomaterials.[103] Yang et al. used a high-intensity pulsed light technique to embed AgNWs into PU and simultaneously improved NW–NW junction conductivity and NW–substrate adhesion, as shown in **Figure 3**a.[112] High density, light-induced extreme local heat in the AgNWs caused the adjacent PU to soften and melt while allowing heavy AgNWs to be embedded into PU without substantial damage to the substrate. The resulting AgNW/PU composite electrodes retained a high electrical conductivity of <10 Ω sq^{-1} even under 100% strain. Recently, AuNWs became an alternative option because of their chemical inertness, biocompatibility, high electrical conductivity, and suitable work function for p-type semiconductors.[113] Bowen et al. obtained vertically aligned AuNWs embedded conductive polydimethylsiloxane (PDMS) with a high conductivity of 1288 S cm^{-1} at 0% and 152 S cm^{-1} at 170% strain.[114] The AuNWs were fabricated by combining both bottom-up synthesis of AuNWs and top-down patterning (Figure 3b). Furthermore, the vertical AuNWs electrodes maintained low ohmic contact with a semiconducting P3HT thin film in a wide strain range (0–100%). Stretchable transistors were demonstrated with little performance degradation up to 100% strain. Carbon nanotubes (CNTs) are also used as conductive fillers, however, the conductivity of CNT-based conductive rubbers were lower than those of metal (Ag, Cu) NWs composites.[115] Chun et al. improved their

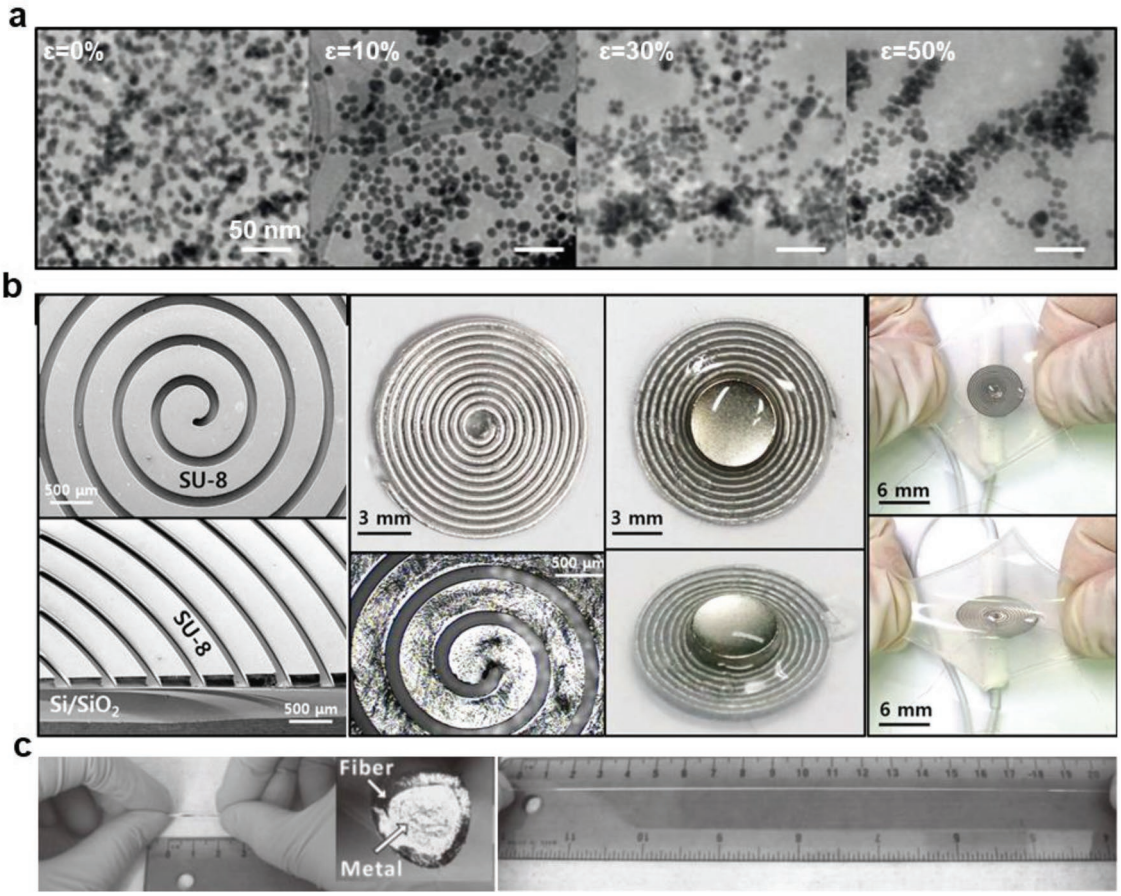

Figure 2. 0D nanomaterial-based rubbery conductors. a) TEM images of NP-based rubbery conductors with self-alignment under different levels of uniaxial strain (from 0% to 50%). Reproduced with permission.[110,111] Copyright 2013, Springer Nature. b) SEM images of SU-8 mold (left), optical images of the microchannel (middle), fabricated SAD with and without stretch (right). Reproduced under the terms and conditions of the CC-BY Creative Commons Attribution 4.0 International License.[72] Copyright 2015, The Authors, published by the Springer Nature. c) A liquid metal filled ultrastretchable conductive fiber stretched 10 times its initial length. Reproduced with permission.[111] Copyright 2013, Wiley-VCH.

conductivity by introducing metallic NPs into a CNTs composite shown in Figure 3c.[98] A highly conductive Ag-multiwalled carbon nanotubes (Ag-MWNT)/polyvinylidene fluoride (PVDF) film was developed by mixing the self-assembled MWNTs decorated by AgNPs, ionic liquid, Ag flakes, and PVDF. The PVDF composite was obtained by drop casting and maintained high conductivity and excellent mechanical robustness (5710 S cm^{-1} at 0% strain and 20 S cm^{-1} at 140% strain).

2D materials including graphene and metallic flakes/sheets have a large junction area, which allows for reduced contact resistance. 2D nanomaterials based rubbery conductors with high stretchability and conductivity have also been investigated. Sunghwan et al. employed AuNSs as fillers to innovate a conductive thermoplastic block copolymer polystyrene-block-polybutadiene-block-polystyrene (SBS) on PDMS (Figure 3d).[116] The nonintrinsically stretchable viscoelastic composite could follow the elastic behavior of the PDMS substrate (up to 180% strain) due to the strong interface between SBS and PDMS. Strong adhesion of SBS to the AuNSs made the composite highly conductive and mechanically durable with the sheet resistance linearly increasing from 0.45 Ω sq^{-1} at 0% strain to 9.4 Ω sq^{-1} at 160% strain. 2D nanomaterials based rubbery conductors can also be obtained by mixing the fillers and rubber. Someya et al. presented a conductive rubber ink comprised of Ag flakes, a fluorine rubber, and a fluorine surfactant (Figure 3e).[117] When adding the fluorine surfactant, the Ag flakes in the printable ink tended to aggregate to form localized conductive networks near the top surface, inducing a high conductivity of 738 S cm^{-1} without strain and 182 S cm^{-1} under 215% strain. The same group further improved this ink by introducing AgNPs in situ formed from inlaid Ag flakes in rubber when heated in an elastomer (Figure 3f).[97] The results showed that with a small fraction of AgNPs, the percolation threshold dramatically decreased from 0.111 to 0.046. Due to the polymer reinforcement effect of AgNPs, or normalization of the stress distribution, the conductive rubbery composite showed a conductivity as high as 6168 S cm^{-1} at 0% strain, and 935 S cm^{-1} when stretched up to 400%.

3. Rubbery Semiconductors

The semiconductor, which determines the electrical properties of transistors, is the most important component in transistors. Traditional semiconductors are mechanically

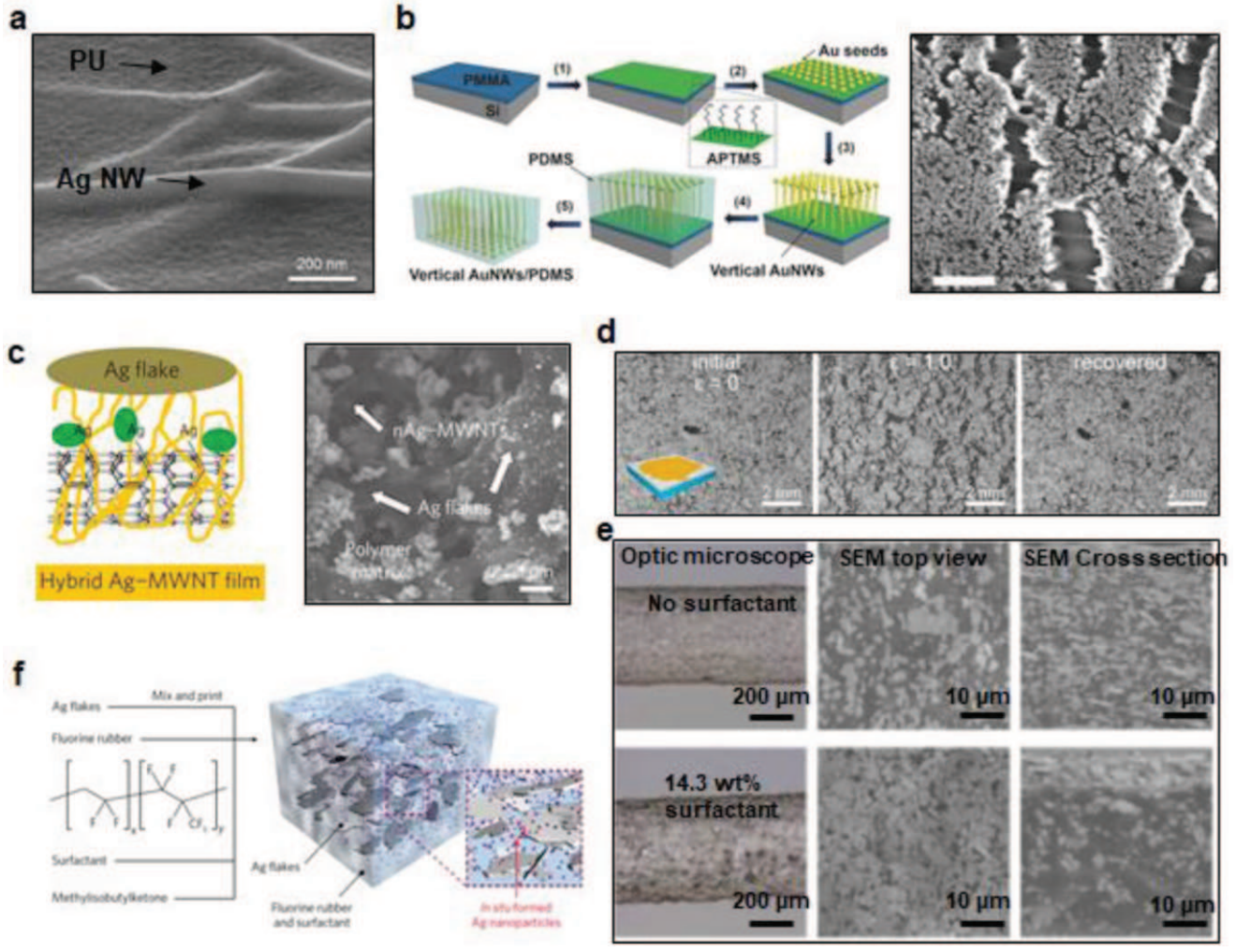

Figure 3. 1D and 2D nanomaterials based rubbery conductors. a) Tilted SEM images of AgNWs/PU composite fabricated by a high density pulsed light technique. Reproduced with permission.[112] Copyright 2016, Springer Nature. b) Schematic of fabrication processes of vertical AuNWs embedded in PDMS films and SEM images of a vertical AuNWs/PDMS composite under 50% strain. Reproduced with permission.[114] Copyright 2019, Wiley-VCH. c) Schematic and SEM image of a hybrid Ag–MWNT composite. Reproduced with permission.[98] Copyright 2010, Springer Nature. d) SEM images of the AuNS/SBS composite film under initial, strained at $\varepsilon = 1.0$ after 100 cycles, and recovered conditions. Reproduced with permission.[116] Copyright 2017, American Chemical Society. e) Optical microscopic and SEM images of micrometer-sized Ag flakes based rubbery conductors with and without surfactants. Reproduced under the terms and conditions of the CC-BY Creative Commons Attribution 4.0 International License.[117] Copyright 2015, The Authors, published by Springer Nature. f) Schematic illustration showing AgNPs synthesized in situ from micrometer-sized Ag flakes. Reproduced with permission.[97] Copyright 2017, Springer Nature.

nonstretchable (rigid and brittle), which restricts the development of technologies such as wearable electronics, biomedical devices, and healthcare systems.[118,119] Most of the efforts to realize stretchable electronics using mechanically nonstretchable semiconductors typically involve implementing structural engineering strategies such as wrinkles,[120–123] kirigami,,[124,125] and microcracks.[126,127] However, those approaches have certain limitations and drawbacks, as discussed before. On the other hand, rubbery semiconductors have drawn increasing interest for constructing stretchable electronics due to their mechanical stretchability and easy fabrication. Here, we categorize rubbery semiconductors into two groups, including intrinsically stretchable polymeric semiconductors and stretchable semiconducting composites based on polymer and elastomer blends.

3.1. Intrinsically Stretchable Polymeric Semiconductors

One straightforward approach to develop stretchable semiconductors is to molecularly design intrinsically stretchable polymeric semiconductors with π-conjugated structures. Typically, electrical and mechanical properties of conjugated polymers can be engineered by modifying the backbone and sidechains to control various factors such as molecular planarity, π-stacking distance, crystallinity, glass transition temperature, interchain interactions, etc.[45,128–132] Molecular backbone engineering is a straightforward and widely used approach to develop a new class of stretchable semiconducting polymers.[37–45] Müller et al. synthesized a semiconducting diblock copolymer using polyethylene (PE) and regioregular P3HT, which had a stretchability higher than 600% based on a PE moiety of 90 wt% (**Figure 4**a)

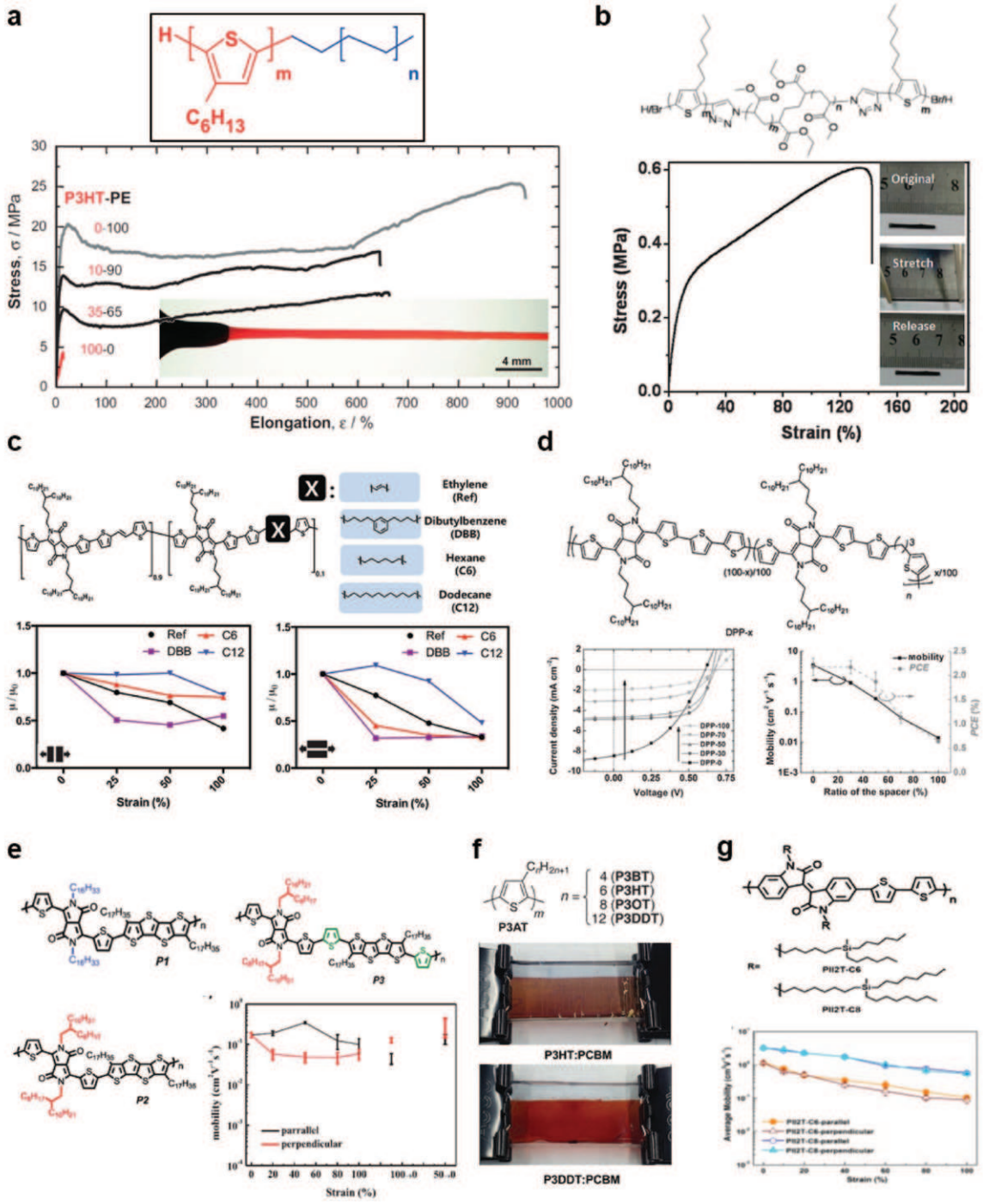

Figure 4. Intrisically stretchable polymeric semiconductors. a) Chemical structure of the P3HT-PE diblock copolymer (top) and stress–strain curves of the film with different ratios of P3HT and PE (bottom). The inset of the bottom image is an optical image of 35–65 P3HT-PE under mechanical strain of 600%. Reproduced with permission.[39] Copyright 2007, Wiley-VCH. b) Chemical structure of triblock copolymer P3HT-PMA-P3HT (top) and stress–strain curves of the polymer. Reproduced with permission.[42] Copyright 2015, Royal Society of Chemistry. c) Chemical structures of DPP-based semiconducting polymers containing 10 mol% of spacers (top) and normalized field-effect mobilities of the polymer films under mechanical strain parallel (bottom, left) and perpendicular (bottom, right) to the channel length direction. Reproduced with permission.[40] Copyright 2018, Wiley-VCH. d) Chemical structure of DPP based polymer with a nonconjugated spacer (top), photovoltaic properties (bottom, left), and photoconversion efficiency (bottom, right) of the polymers. Reproduced with permission.[44] Copyright 2016, Wiley-VCH. e) Chemical structures of three different thiophene DPP-based polymers and the mobility of the P3 based transistor. Reproduced with permission.[38] Copyright 2017, Wiley-VCH. f) Chemical structures of P3HT with different sidechains (top), optical images of P3HT:PCBM and P3DDT:PCBM films under mechanical strain. Reproduced with permission.[46] Copyright 2014, Wiley-VCH. g) Chemical structure of PII2T based polymer with different lengths of a carbosilane sidechain (top) and field-effect mobilities of the polymer thin films under various strain levels (bottom). Reproduced with permission.[50] Copyright 2016, American Chemical Society.

and a field effect mobility of 0.02 cm^2 V^{-1} s^{-1} was obtained from the transistor based on those materials.[39] The effect of introducing a soft PE block into the backbone on mechanical properties is substantial, especially when considering the fracture strain of P3HT (≈13%). As another example of molecular backbone engineering, Peng et al. developed an ABA triblock copolymer for a stretchable semiconductor using P3HT as A and poly(methyl acrylate) (PMA) as B to form a P3HT-PMA-P3HT triblock copolymer.[42] The novel semiconductor–rubber–semiconductor structure demonstrated a field effect mobility of 9×10^{-4} cm^2 V^{-1} $s^{-1}$with a high stretchability of 140% (Figure 4b). Another approach to enhance mechanical softness is to introduce a spacer into the molecular backbone of the polymer to reduce crystallinity and the glass transition temperature (T_g).[38,40,41,44] As shown in Figure 4c, Mun et al. examined the effect on mechanical properties of a semiconducting polymer by inserting a nonconjugated spacer into the molecular backbone.[40] Three different spacers were introduced into the backbone of a diketopyrrolopyrrole (DPP) based polymeric semiconductor to show that the longer chains acting as spacers in the backbone resulted in a lower modulus and better stretchability due to greater flexibility of the molecules. Savagatrup et al. used an aliphatic propyl chain as a spacer in the DPP based polymer backbone to improve ductility and reduce the modulus.[44] Although the photo conversion efficiency of a photovoltaic cell and the field effect mobility of a transistor decreased with an increasing amount of nonconjugated units, the results clearly emphasized that mechanical properties can be modulated by controlling the portion of the spacer in the backbone (Figure 4d). Since the sidechains also affect physical properties of molecules, Lu et al. investigated the effect of both the backbone and sidechains on the mechanical stretchability of the polymer poly(tetrathienoacene-diketopyrrolopyrrole) (PTDPPTFT4) and its two analogs with different branched alkyl sidechains and a thiophene spacer inserted into the backbone (Figure 4e).[38] The thiophene inserted polymer showed a higher crack onset strain with a stable mobility of 0.1 cm^2 V^{-1} s^{-1} under a mechanical strain of 100%. The branched alkyl chain induced a lower T_g and a higher crack onset strain compared to PTDPPTFT4, which resulted from more amorphous regions in the polymer film with branched chains than those in the PTDPPTFT4 film. Thus, sidechain engineering of polymeric semiconductors is critical due to its substantial effect on the mechanical properties of the polymer.[46–50,130] Savagatrup et al. reported mechanical properties of poly(3-alkylthiophene) (P3AT) depending on just the length of the sidechain maintaining the structure of the backbone.[46] Longer sidechains reduced the modulus of both the P3AT film alone and the blended film containing P3AT and phenyl-C_{61}-butyric acid methyl ester (PCBM). While the photovoltaic cell based on P3HT and PCBM did not function under a mechanical strain of 10% (obvious cracks were in the film), poly(3-dodecylthiophene) (P3DDT) and PCBM based devices presented no significant degradation under 10% strain: there were no visible cracks as shown in Figure 4f. Wu et al. also investigated the sidechain effect using an isoindigo-based conjugated polymer, polyisoindigobithiophene (PII2T), with two carbosilane sidechains of different lengths.[50] Both polymers showed stable charge transport properties under a mechanical strain of 100% (Figure 4g).

3.2. Stretchable Semiconducting Composites

Other facile approaches to enable the mechanical stretchability in semiconducting materials are to form composites by blending two or more semiconducting polymers with different properties or by mixing semiconducting fillers with rubbers. These approaches have advantages such as easy engineering of composite properties and the capability to achieve infinite combinations from various polymers.

Blending has been explored in order to utilize the high charge transport property of one conjugated polymer and the desirable mechanical properties of another conjugated polymer.[43,51–53] Savagatrup et al. blended P3ATs with different alkyl chains and successfully decreased the modulus while optimizing both the electrical and mechanical performances (**Figure 5**a).[43] Using a similar approach, Scott et al. created a conjugated polymer blend for a stretchable semiconductor consisting of the polymers poly[4-(4,4-dihexadecyl-4H-cyclopenta[1,2-b:5,4-b′]dithiophen-2-yl)-alt-[1,2,5]thiadiazolo[3,4-c]pyridine] (PCDTPT) and P3HT.[52] The field effect transistor based on the blend (PCDTPT:P3HT = 1:1) showed a good field effect mobility of 0.8 cm^2 V^{-1} s^{-1}, which is similar to that of a device only based on PCDTPT (0.9 cm^2 V^{-1} s^{-1}) (Figure 5b). Depending on the applied strain, the mobility increased due to the polymer backbone alignment in the strain direction (channel length direction).[54]

Another blending approach involves combining conjugated polymers and nonconjugated polymers (i.e., insulating polymer) to form rubbery semiconductor composites. To exploit the superior mechanical softness of the nonconjugated polymer used for the rubbery semiconducting layer, various combinations of blending have been developed.[55–65,133] Because nonconjugated polymers are insulators, the semiconductor should be percolated when mixed to form an electrical pathway while maintaining the mechanical advantages of the nonconjugated polymer.[57,60] Blending conjugated polymers and nonconjugated polymers to tune the mechanical properties of the composite is a technique that has been used for decades. In 1992, Moulton used poly(3-octylthiophene) (P3OT) and high molecular weight PE to develop a polymer composite; P3OT gave the composite increased conductivity while PE made the composite soft.[61] Although this blending technique to prepare rubbery semiconductors has been known, it has more recently invited attention due to the rising interest in stretchable electronics. Among many insulating elastomers, PDMS is one of the widely used materials to fabricate rubbery semiconductor composites through this blending approach.[59–61,64,66,133] Song et al. reported a blend containing prepared P3HT NWs (P3HT-NWs) in PDMS for a stretchable semiconductor.[66] They found that the phase separation of P3HT-NWs and the PDMS matrix depends on the surface characteristics of the substrate, and therefore, P3HT-NWs could be uniformly percolated in PDMS substrates. Even 1 wt% P3HT in PDMS could be used as the semiconductor for field effect transistors and the devices showed more stable operation under mechanical strain up to 100% than devices based only on P3HT (**Figure 6**a). Similarly, Kim et al. prepared P3HT nanofibrils (P3HT-NFs) by heating (60 °C) and cooling (−20 °C) for self-assembled, highly crystalline P3HT-NFs to blend with PDMS for fully rubbery electronics and sensors (Figure 6b).[59] SEBS has also been recently used

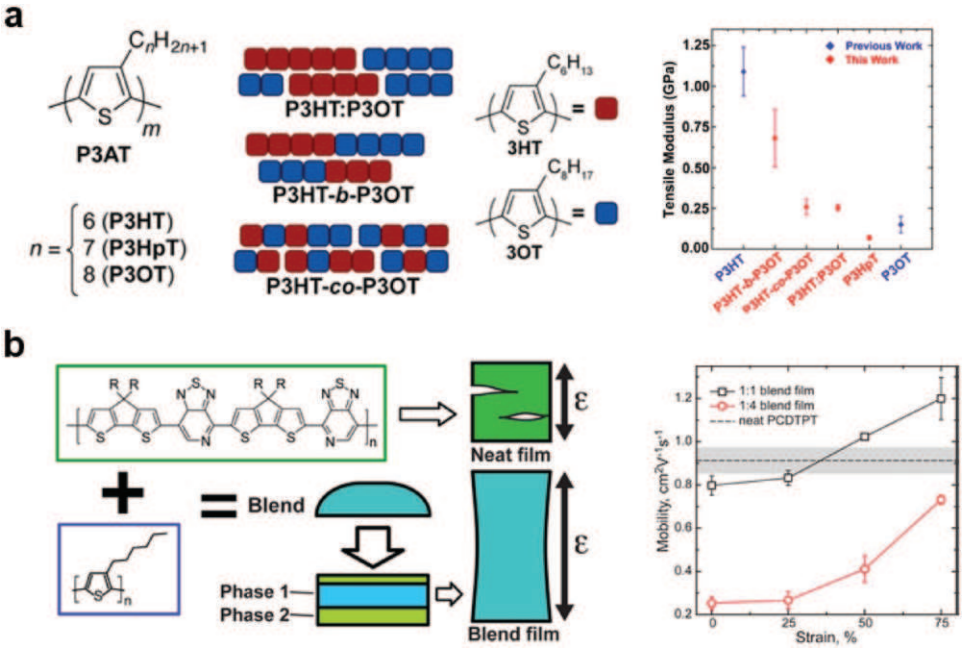

Figure 5. Stretchable semiconducting composites from blending different conjugated polymers. a) Chemical structures/schematic diagrams of the organic semiconductors (left) and plot of the tensile modulus (right). Reproduced with permission.[43] Copyright 2014, American Chemical Society. b) Schematic diagram of the film formation with chemical structures of the polymers (left) and saturated field effect mobilities in the blend films with applied strain for charge transport parallel to the strain direction. Reproduced with permission.[52] Copyright 2016, American Chemical Society.

as an elastomer for stretchable electronics because of its superior mechanical softness, as demonstrated by Shin et al.'s use of P3HT and SEBS as a rubbery semiconductor composite (Figure 6c).[63,65,133] They used the blend after cooling (−15 °C) and warming (25 °C) before spin casting to form a high quality P3HT-NF film. Aside from P3HT, other semiconducting materials have been utilized. Another conjugated polymeric semiconductor, poly(2,5-bis(2-octyldodecyl)-3,6-di(thiophen-2-yl) diketopyrrolo[3,4-c] pyrrole-1,4-dione-alt-thieno[3,2-b]thiophen) (DPPT-TT), was used with 70 wt% SEBS to form a rubbery semiconductor composite through the nanoconfinement effect (Figure 6d).[65] The resulting film had improved mechanical properties and maintained its electrical characteristics under not only mechanical stretching in both the horizontal and vertical directions, but also for various deformations such as twisting and poking. Four additional different conjugated polymers for stretchable semiconductors were used as alternatives to the aforementioned polymeric semiconductor, proving that their approach could be utilized for other materials. Thus, their results emphasized the improvement in mechanical properties through increasing the chain dynamics and decreasing the crystallinity of the polymer embedded in SEBS.

Occasionally, polymer blends induce vertical phase separation of the semiconducting polymer and insulating layer during coating and annealing due to the difference in surface energy and solubility parameters. Several studies on organic field effect transistors exploited this concept to form bilayered structures (semiconductor/dielectric) in a one-step process.[67,68] Most studies focused on devices on rigid substrates, but Zhang et al. recently demonstrated fully rubbery electronic devices based on vertical phase separation to form a stretchable semiconducting layer and PDMS dielectric layer in a single step (Figure 6e).[69] The vertical phase separation induced an interpenetrating polymer network on one side, which created a percolation network even with a small concentration of a semiconducting polymer. Three different semiconducting polymers were used including P3HT, poly[2,5-(2-octyldodecyl)-3,6-diketopyrrolopyrrole-alt-5,5-(2,5-di(thien-2-yl)thieno [3,2-b]-thiophene)] (DPP-DTT), and poly(2,5-bis(2-octyldodecyl)-3,6-di(pyridin-2-yl)-pyrrolo[3,4-c]pyrrole-1,4(2H,5H)-dionealt-2,2′-bithiophene) (DPPDPyBT). Their transistor, which was based on a blend of the three polymers as the semiconductor with low weight fractions (f_{P3HT} = 0.49%, $f_{DPP\text{-}DTT}$ = 0.83%, and $f_{DPPDPyBT}$ = 0.62%), demonstrated adequate performance and mechanical durability under 100% strain.

4. Rubbery Dielectrics

To achieve mechanically durable rubbery electronics, the rubbery dielectric is also a critical component since the dielectric plays an important role in field effect transistors. It controls the current flow between the source and drain electrodes by applying an electrical potential across the source and gate electrodes. Various approaches such as wrinkled oxides for stretchable transistors were developed.[25,67,121,134] As an example, Chae et al. investigated randomly wrinkled Al_2O_3 as gate dielectrics for the stretchable transistors, which displayed no substantial performance degradation under a mechanical strain of 20%.[134] However, those approaches based on structural engineering cannot easily achieve low cost and simple manufacturing. Therefore, the development of rubbery dielectrics is urgent, and several materials have already been proposed. The rubbery dielectric can be categorized into two groups: elastomers and ion gels.

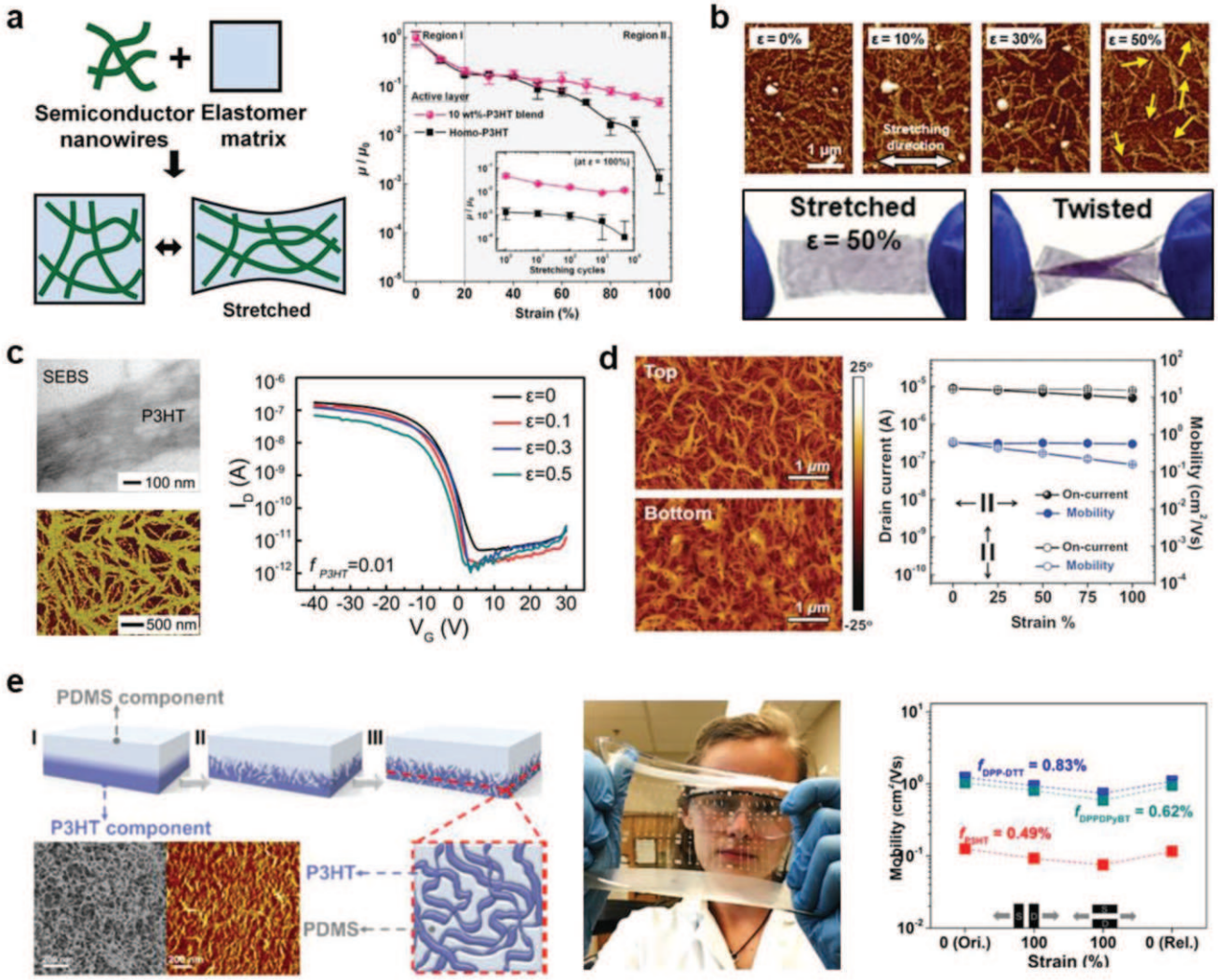

Figure 6. Stretchable semiconducting composites from blending conjugated polymers with nonconjugated polymers. a) Schematic illustration of the stretchable organic semiconductor preparation (left) and the homo-P3HT TFT and 10 wt% P3HT blend TFT device performances depending on mechanical strain (right). Reproduced with permission.[66] Copyright 2016, Wiley-VCH. b) AFM images of the stretchable P3HT-NF/PDMS semiconductor spin-coated on a PDMS substrate (top) and the film under various mechanical deformations (right). Reproduced under the terms and conditions of the CC-BY-NC Creative Commons Attribution NonCommercial License 4.0.[59] Copyright 2017, The Authors, published by American Association for the Advancement of Science. c) Representative TEM image (left, top), a phase-mode AFM image (left, bottom) of a P3HT-NFs bundle indented in the SEBS, and transfer curves of 1 wt% P3HT blend TFT device under different mechanical strains (right). Reproduced with permission.[63] Copyright 2015, Wiley-VCH. d) AFM phase images of the top and bottom interfaces of the rubbery semiconductor composite film with 70 wt % SEBS (left) and changes in the on current and mobilities with strains up to 100%, both parallel to (filled circles) and perpendicular to (open circles) the charge transport direction (right). Reproduced with permission.[65] Copyright 2017, American Association for the Advancement of Science. e) Schematic illustration of formation and SEM and AFM images of the IPN structure (left), photograph of the transparent transistor arrays with strain (middle), and mobility changes of the transistor under 0%, 100% strain, and after release (right). Reproduced with permission.[69] Copyright 2017, American Chemical Society.

4.1. Elastomers

An elastomer is an excellent option for a stretchable gate dielectric because of its superior mechanical durability and easy fabrication by using conventional processes such as spin-casting. For example, PDMS, a traditionally well-known elastomer, was used as the gate dielectric for the fabrication of transistors.[41,135–140] Oh et al. used transferred PDMS as the gate dielectric to develop a stretchable transistor with healable semiconducting materials (**Figure 7**a).[41] The devices withstood a mechanical strain of 100% both along and perpendicular to the channel length directions, even after a 100 cycle stretching test. Even though PDMS has superior mechanical properties, its relatively low dielectric constant (≈2.7)[141] limits the device performance. To overcome this limitation, hybrid elastomer gate dielectrics were developed.[142–146] Cai et al. used barium titanate ($BaTiO_3$) NPs to form a hybrid composite with PDMS, resulting in a high dielectric constant (≈9 at ≈26 vol% $BaTiO_3$) of the composite

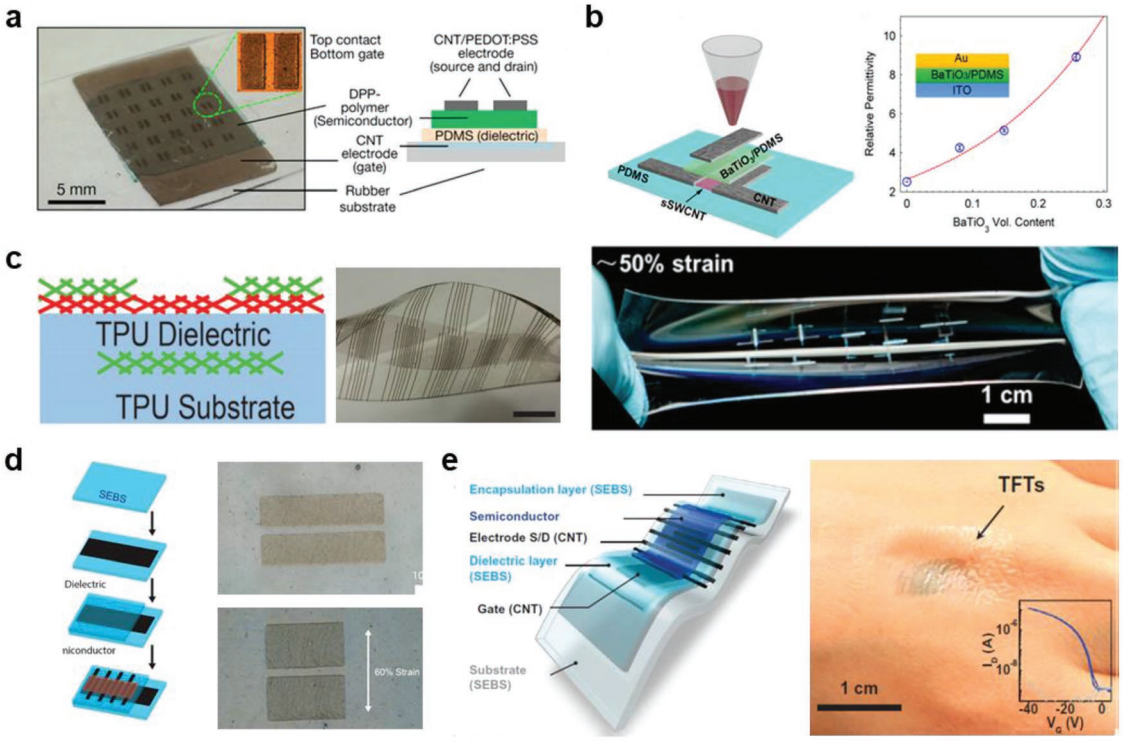

Figure 7. Elastomers. a) Photograph of a fully stretchable 5 × 5 organic transistor array (left) and the architecture of a single transistor with PDMS dielectric (right). Reproduced with permission.[41] Copyright 2016, Springer Nature. b) Schematic illustration of a printed stretchable TFT with $BaTiO_3$/PDMS composite as the gate dielectric (left), relative permittivity of the $BaTiO_3$/PDMS composite with various volume contents of $BaTiO_3$ NPs (right), and an image of a 50% stretched device (bottom). Reproduced with permission.[142] Copyright 2016, American Chemical Society. c) Schematic illustration of a thermoplastic PU (TPU) gated transistor (left) and an image of the twisted device (right). Reproduced with permission.[147] Copyright 2015, Wiley-VCH. d) Transfer process for devices with SEBS dielectric (left) and images of unstrained and 60% stretched devices (right). Reproduced with permission.[148] Copyright 2017, American Chemical Society. e) Schematic illustration (left) showing SEBS gated fully stretchable transistor with skin-like nature when attached to the back of a hand (right). Reproduced with permission.[65] Copyright 2017, American Association for the Advancement of Science.

material (Figure 7b).[142] PU is also one of the widely used elastomers for stretchable field effect transistors[36,127,147] because of its good mechanical stretchability and relatively high dielectric constant (≈6.2).[141] Chortos et al. fabricated a CNT based transistor using thermoplastic PU (TPU) as the gate dielectric to retain its functionality under mechanical deformations such as physical impacts, punctures, and tears (Figure 7c).[147] The higher toughness and tear strength of the TPU, compared to the commonly used PDMS, not only enabled the device to maintain its functionality under mechanical stretching over 1000 cycles, but also increased its resistance to mechanical damage. The nonpolar elastomer dielectric material, SEBS, was used for stretchable transistors because of its low concentration of dipoles which minimizes hysteresis.[65,140,148–150] Chortos et al. used SEBS as an elastomer gate dielectric to investigate the band-gap effect of single-walled carbon nanotubes (SWNTs) on transistor performance.[148] The fabricated devices exhibited negligible hysteresis and operated normally under a mechanical strain of 60% (Figure 7d). Xu et al. also implemented SEBS as a gate dielectric and reported the nanoconfinement of a polymer semiconductor based highly stretchable transistor (Figure 7e).[65] Besides the abovementioned specific examples, cross-linked polymers have also been used for stretchable gate dielectrics.[141,149,151]

4.2. Ion Gels

Ion gel contains ionic liquid inside of a porous polymeric matrix and is another type of gate dielectric, which brings several advantages such as a large specific capacitance and mechanical deformability. Ionic liquid, the key component of ion gel, is in a liquid state at room temperature with a high ionic conductivity, extremely low vapor pressure, and high chemical/thermal stability.[152–154] However, further usage of ionic liquid is limited due to the physical properties of the liquid phase at room temperature. Therefore, mixing ionic liquid into a polymeric matrix was developed for ion gel due to its immobilized phase while keeping the advantages of the ionic liquid. The working mechanism of ion gel in field effect transistors is different from the conventional solid-state gate dielectric. Under an electric field across the ion gel, a thin electric double layer is formed at both interfaces (between the ion gel/semiconductor and the ion gel/gate electrode) which leads to a high capacitance at the interfaces.[155–157] Based on those advantages, ion gel was widely used for not only rigid field effect transistors,[158–165] but also various stretchable electronics.[59,64,133,166–168]

As an example, Lee et al. developed a stretchable graphene transistor by using ion gel as the gate dielectric made from poly(styrene-methyl methacrylate-styrene) (PS-PMMA-PS)

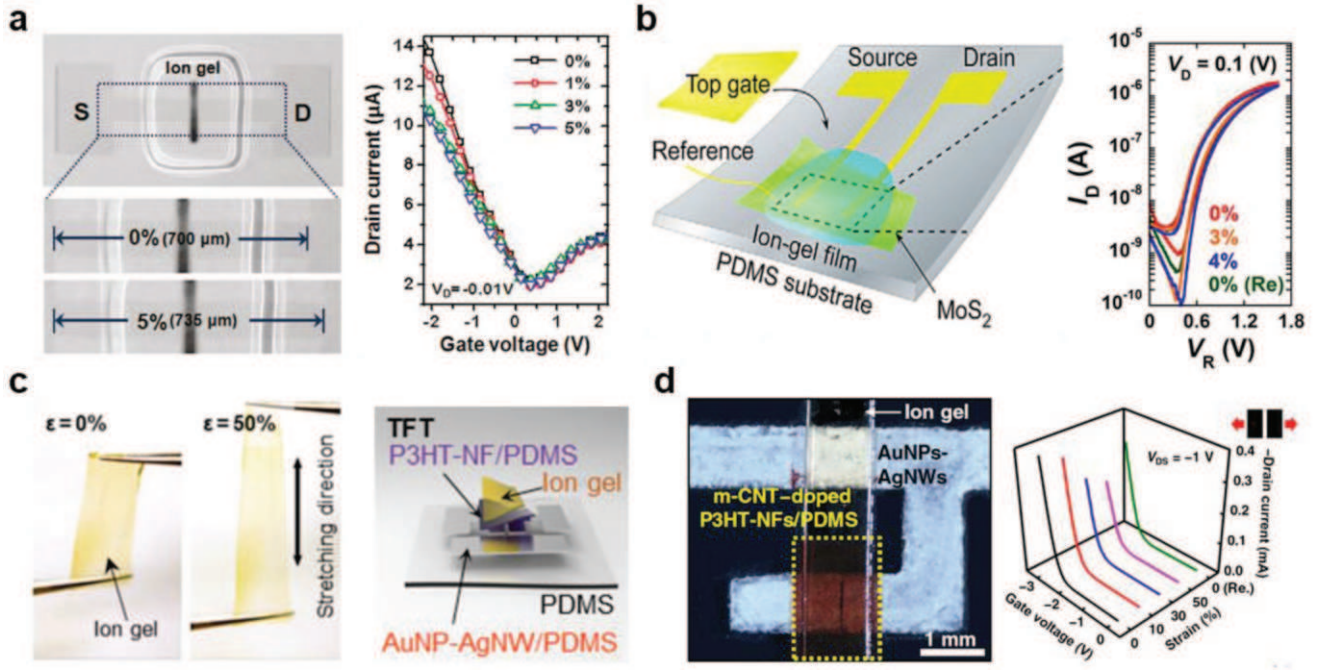

Figure 8. Ion-gel gated transistors. a) Microscope images of trilayer graphene FETs with ion gel dielectric under 5% strain along the longitudinal direction of the channel (left) and a typical transfer curve of stretched graphene FETs on PDMS substrate (right). Reproduced with permission.[166] Copyright 2011, American Chemical Society. b) Schematic depiction of an MoS_2 TFT with the triblock copolymer and the ionic liquid (left), and transfer characteristics of the MoS_2 TFTs under various strains (right). Reproduced with permission.[167] Copyright 2011, American Institute of Physics. c) Images of a free-standing ion gel dielectric before and after 50% stretching (left) and schematic illustration of an ion gel gated TFT (right). Reproduced under the terms and conditions of the CC-BY-NC Creative Commons Attribution NonCommercial License 4.0.[59] Copyright 2017, The Authors, published by the American Association for the Advancement of Science. d) Optical image (left) and transfer characteristics under different mechanical strains along the channel length direction (right) of a PVDF-HFP/EMIM-TFSI based ion gel gated rubbery transistor. Reproduced under the terms and conditions of the CC-BY-NC Creative Commons Attribution NonCommercial License 4.0.[64] Copyright 2019, The Authors, published by the American Association for the Advancement of Science.

triblock copolymer as the matrix and 1-ethyl-3-methylimidazolium bis(trifluoromethylsulfonyl)imide (EMIM-TFSI) as the ionic liquid: the transistor showed a high hole mobility of 1188 $cm^2\ V^{-1}\ s^{-1}$ with 5% stretchability (**Figure 8**a).[166] Similarly, an MoS_2 based stretchable transistor with a maximum stretchability of 5% was reported using the same ion gel (Figure 8b).[167] Other combinations of a polymer matrix and ionic liquid have been reported. Kim et al. used poly(vinylidene fluoride-co-hexafluoropropylene) (PVDF-HFP) as the polymeric matrix with the ionic liquid 1-ethyl-3-methylimidazolium trifluoromethanesulfonate (EMIM-Oft) for a fully rubbery transistor (Figure 8c).[59] Sim et al. combined PVDF-HFP and EMIM-TFSI for ion gel to create high mobility rubbery transistors and introduced metallic CNTs into the semiconducting layer (Figure 8d).[64]

5. Rubbery Electronics

Stretchable electronics have tremendous potential for future applications such as wearable electronics, artificial skins, biomedical devices, etc. Because structural engineering for stretchable electronics with intrinsically nonstretchable materials has limitations for integration, packaging, and manufacturing cost due to large space usage for interconnection, stretchable electronics based on all rubber-like components are promising future alternatives. Therefore, many rubbery electronics have been developed including transistors, logic gates, optoelectronic devices, physical sensors, energy harvesting devices, and others.[41,52,59,60,64,65,99,133,169–192]

5.1. Rubbery Transistors and Integrated Electronics

The rubbery transistor is one of the urgently required devices for an advanced rubbery electronics system because the transistor is the basic component for various electronic systems. Therefore, many studies on rubber-like stretchable transistors and integrated electronics have been actively conducted.[41,52,59,64,65,133,169] Kim et al. developed fully rubbery electronic materials including P3HT-NFs percolated in PDMS as the rubbery semiconductor, AgNWs embedded in PDMS as the electrodes, and ion gel as the gate dielectric; these rubbery materials were used to construct uniaxially stretchable (**Figure 9**a)[59] and biaxially stretchable transistors (Figure 9b).[133] It is noted that gold NPs (AuNPs) were coated on top of AgNWs to minimize the energy barrier between the source/drain electrodes and the semiconducting layer. As shown in Figure 9c, Sim et al. recently realized high-mobility, intrinsically stretchable semiconductor based fully rubbery transistors as more advanced versions of the previously

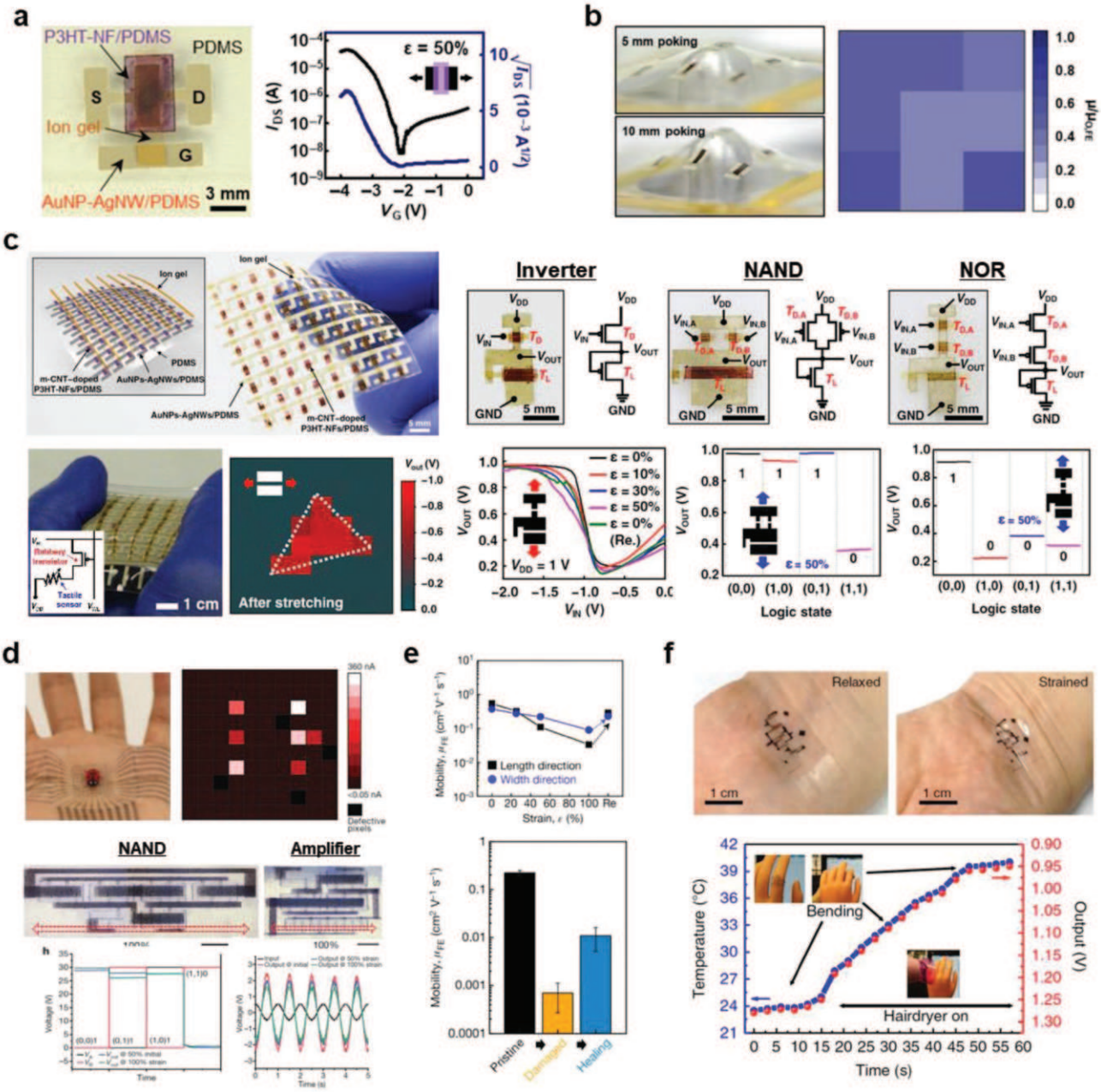

Figure 9. Rubbery transistors and integrated electronics. a) Optical image of a fully rubbery transistor (left) and its transfer performance under 50% strain along the channel length direction (right). Reproduced under the terms and conditions of the CC-BY-NC Creative Commons Attribution NonCommercial License 4.0.[59] Copyright 2017, The Authors, published by the American Association for the Advancement of Science. b) Tilted views of the biaxially stretchable rubbery transistor array that was poked by a pin with different poking distances and the mapped mobilities of the transistor array under poking with 10 mm distance. Reproduced with permission.[133] Copyright 2018, Wiley-VCH. c) An optical image of the fabricated high-performance rubbery transistors array (left, top), optical images/mapping result of fully rubbery tactile sensing skin (left, bottom), and optical image/electrical characteristics of logic gates (right). Reproduced under the terms and conditions of the CC-BY-NC Creative Commons Attribution NonCommercial License 4.0.[64] Copyright 2017, The Authors, published by the American Association for the Advancement of Science. d) High density stretchable transistor array adhered and conformed to a human palm performed electrical detection of six conductive legs of a synthetic ladybug (top) and optical microscope images/output–input characteristics of the intrinsically stretchable NAND and amplifier without and with 100% strain (bottom). Reproduced with permission.[193] Copyright 2018, Springer Nature. e) Field-effect mobility of a stretchable transistor during a stretching cycle (top) and a damage-healing cycle (bottom). Reproduced with permission.[41] Copyright 2016, Springer Nature. f) Optical photographs of a stretchable strain-independent temperature sensor conformally integrated on a wrist (top) and its stable performance during repeated bending deformations (bottom). Reproduced with permission.[169] Copyright 2018, Springer Nature.

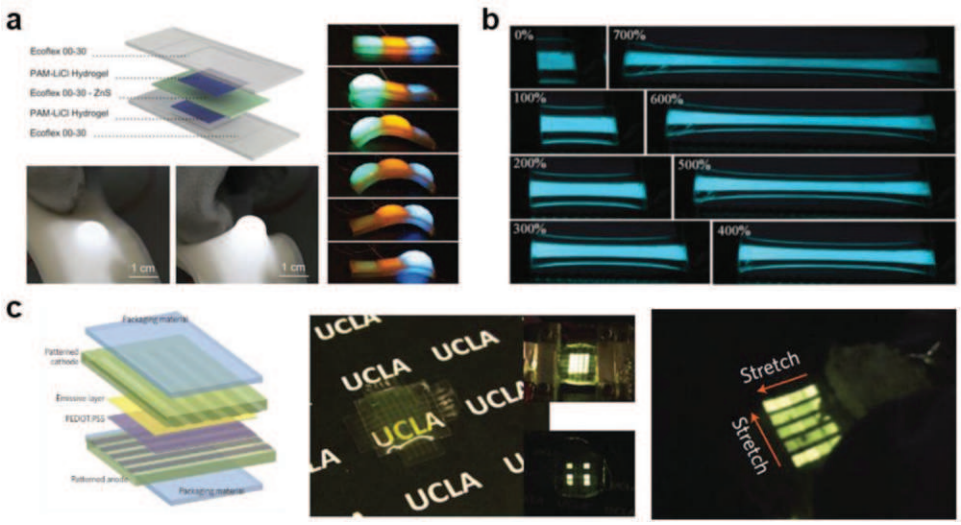

Figure 10. Rubbery optoelectronics. a) Schematic illustration showing the structure of the hyperelastic light-emitting capacitor (HLEC) and images of the stretchable HLEC wrapped around the end of a pencil (left) and a soft robot that can dynamically change its color based on external and internal stimuli (right). Reproduced with permission.[170] Copyright 2016, American Association for the Advancement of Science. b) Photographs of the electroluminescent device under various strains. Reproduced with permission.[172] Copyright 2015, Wiley-VCH. c) Schematic illustrations of an encapsulated fully stretchable EPLED display comprising 5 × 5 pixels (left) and demonstrations of EPLED displays in flattened (middle) and stretched (right) states. Reproduced with permission.[99] Copyright 2018, Springer Nature.

developed electronics.[64] The transistors showed 9.76 $cm^2 V^{-1} s^{-1}$ as the highest mobility with an average value of 7.30 $cm^2 V^{-1} s^{-1}$ and operated stably under a mechanical strain of 50% for both directions. Fully rubbery logic gates including an inverter, NAND, and NOR gates were fabricated. The logic gates operated normally under a mechanical strain of 50% for both directions. As a further application, a fully rubbery tactile sensing skin with an 8 × 8 active matrix was demonstrated and the tactile mapping capability remained after stretching. In addition, Wang et al. designed a high-density (347 transistors cm^{-2}) stretchable transistor array using a photo patternable gate dielectric, a confinement semiconductor, and CNT electrodes on SEBS.[193] Based on their approach, they demonstrated a 10 × 10 tactile sensor array by using a combination of stretchable transistors and resistive tactile sensors based on two terminal interdigitated CNT electrodes for each pixel. Furthermore, they also characterized a stretchable inverter, NAND gate, and an amplifier (Figure 9d). All demonstrated stretchable electronics functioned normally under a mechanical strain of 100%. Oh et al. also developed rubber-like stretchable transistors from all stretchable components.[41] They used a semiconducting DPP-based polymer with a non-conjugated spacer in the backbone to ensure better mechanical softness as described in section 5. PDMS was used as a stretchable gate dielectric and a spray-coated PEDOT:PSS (30 nm)/CNT (70 nm) bilayer was utilized as the stretchable electrodes. The fabricated rubbery transistors showed a field effect mobility around 0.2 $cm^2 V^{-1} s^{-1}$ and the damaged devices ($\approx 8 \times 10^{-4}$ $cm^2 V^{-1} s^{-1}$) were successfully healed (0.01 $cm^2 V^{-1} s^{-1}$) through solvent vapor and thermal treatment (Figure 9e). In addition, the device performance remained consistent after 100 cycles at a mechanical strain of 100% for both directions. Zhu et al. demonstrated another case of rubbery circuits by constructing a CNT transistor for a stretchable temperature sensing circuit with strain suppression.[169] Because they utilized a stretchable transistor, the strain effect on temperature sensing was minimized to improve the accuracy and robustness of temperature sensing. The transistor is composed of a SEBS substrate and gate dielectric, unsorted SWNTs for the electrodes, sorted SWNTs for the semiconductor, and stretchable PEDOT:PSS as the interconnection. The rubber-like stretchable circuit achieved low inaccuracies of ±1 °C under a mechanical strain range of 0–60% (Figure 9f).

5.2. Rubbery Optoelectronics

Rubbery optoelectronic devices including light emitting devices (electrical-to-optical) and photodetectors (optical-to-electrical) are part of a critical group of electronics used for various applications such as stretchable displays and imaging systems. Two approaches are widely used for rubbery light emitting devices, including a phosphor-doped dielectric[170–173] and a polymer blend[99,169,174] as the light emissive layer. Larson et al. devised a highly stretchable electroluminescent skin with a ZnS phosphor-doped elastomer.[170] A five-layered device consisted of a ZnS-Ecoflex based electroluminescent layer sandwiched between two polyacrylamide-LiCl based hydrogel electrodes, and Ecoflex encapsulation layers at the bottom and top of the device (**Figure 10**a). The devices illustrated high stretchability as they could withstand a mechanical (uniaxial) strain of 395%. Using illuminance and capacitance change under deformation, they demonstrated a soft robot that can dynamically change its color based on external and internal stimuli. Wang et al. employed a similar approach: they embedded ZnS:Cu microparticles in PDMS as the emissive layer by mixing them in a liquid state.[172] The devices with the ionic conductor as the electrodes maintained their light emitting properties under a mechanical strain up to 700% due to the superior mechanical stretchability of the electrodes (Figure 10b). In addition, the authors highlighted the

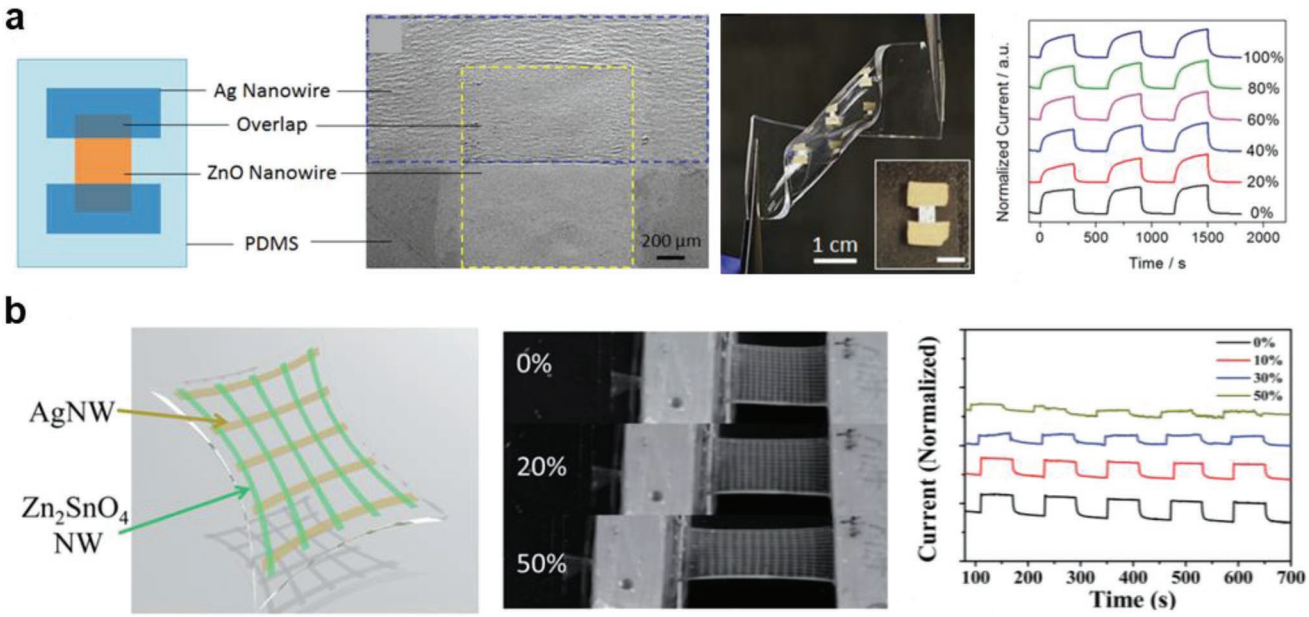

Figure 11. Rubbery photodetectors. a) Schematic illustration and SEM image of a photodetector (left). Image of a stretchable photodetector array on PDMS substrate under twisted condition (middle), and dynamic photo response of the photodetectors under various strains (right). Reproduced with permission.[194] Copyright 2013, Wiley-VCH. b) Schematic illustration of the stretchable transparent UV photodetector (left). Image of the stretchable UV photodetector under different stretching conditions (middle), and dynamic photo response of the photodetectors under various strains (right). Reproduced with permission.[195] Copyright 2014, Royal Society of Chemistry.

mechanical stability of the devices through a cyclic stretching test under 400% strain for 1000 cycles and the devices maintained ≈85% emission intensity. Besides such inorganic light emitting materials, Liang et al. developed organic and elastomeric light emitting devices using an electroluminescent polymer blending layer.[99] To ensure better mechanical softness, a high molecular weight Super Yellow was chosen for a yellow light emitting polymer. The rubber-like emissive layer was formed by blending Super Yellow, ethoxylated trimethylolpropanetriacrylate (ETPTA), polyethylene oxide (PEO), and lithium trifluoromethane sulphonate (LiTf). The device was fabricated in an all solution-based process with PEDOT:PSS coated AgNWs embedded in rubbery poly(urethane acrylate) electrodes. As a result, the device exhibited rubbery elasticity with normal light emission under a mechanical strain of 120%. To confirm the scalability of their approach, a 5 × 5 simple passive matrix monochrome display was demonstrated (Figure 10c).

Another rubbery optoelectronic device that can transduce optical signals into electrical signals is the stretchable photodetector. Because of its promising potential for future applications, many researchers are interested in deformable photodetectors, but the development is limited. Yan et al. introduced a fully rubbery photodetector by using an intrinsically stretchable, light sensing layer based on an NW-embedded elastomer.[194] First, AgNW was patterned on the fully cured PDMS substrate using a PDMS mask, followed by patterning of ZnO NWs by another PDMS mask. Then, liquid PDMS was poured, cured, and peeled off from the substrate to create a fully embedded structure. The devices responded to UV light and the responsivity was retained under a mechanical strain of 100% (**Figure 11**a). Wang et al. also used a similar approach to fabricate a transparent rubbery UV detector using Zn_2SnO_4 NWs as the sensing layer and AgNW/PDMS as the electrodes.[195] As shown in Figure 11b, the devices responded to UV light under a mechanical strain of 50%.

5.3. Rubbery Sensors

Stretchable physical sensors that can be mechanically deformed have tremendous potential for wearable electronics, biomedical devices, and prosthetic skins. Specifically, rubbery physical sensors are superior to their conventional counterparts due to their mechanical compatibility with the soft human body and their simple manufacturing processes. Various rubbery physical sensors have been developed, including pressure sensors,[175–182] strain sensors,[60,180,181,183–187] and temperature sensors.[59,169,188,189]

Jung et al. developed a resistive pressure sensor based on a porous MWNTs/PDMS composite (**Figure 12**a). The porosity of the pressure sensor can be controlled by a solution of reverse micelles that was prepared by mixing an emulsifier, water, and an organic solvent.[175] Moreover, the pressure sensitive rubber can be patterned by a simple fabrication process such as nozzle jet printing as a straightforward demonstration of wearable human–machine interface devices. Boutry et al. recently reported a pressure sensor with a high sensitivity and a fast response time using all stretchable and biodegradable materials.[177] To ensure both stretchability and biodegradable properties, poly (glycerol sebacate) (PGS), poly (octamethylene maleate (anhydride) citrate) (POMaC), and polylactic acid (PLLA) were used for the dielectric layer, packaging, and substrate layer for the magnesium electrode, respectively. The pressure sensor can detect 12 Pa from a grain of salt (Figure 12b). The author demonstrated the biocompatibility of the electrode through an in vivo study. Qin et al. developed another type of pressure

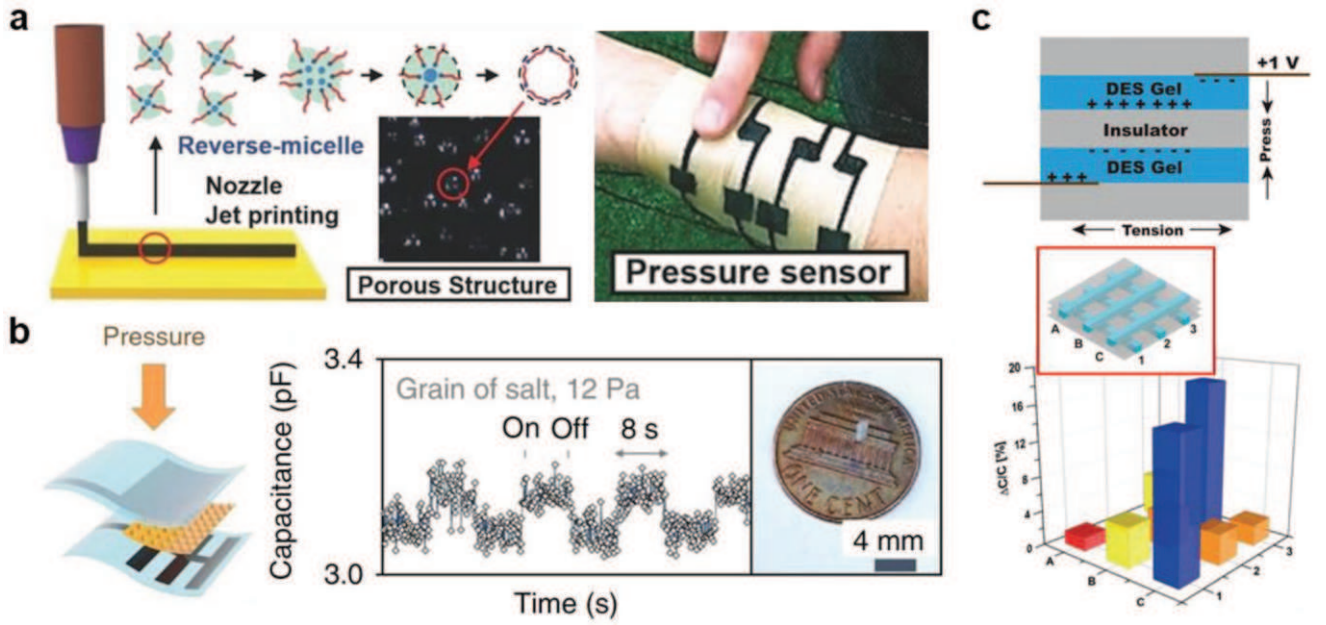

Figure 12. Rubbery pressure sensors. a) Schematic illustration of fabrication for porous pressure-sensitive rubbers by the nozzle jet printing method (left) and the image of the pressure sensor wrapped on the forearm (right). Reproduced with permission.[175] Copyright 2014, Wiley-VCH. b) Schematic view of a pressure sensor (left) and dynamic responsive curve from detecting a grain of salt (right). Reproduced with permission.[177] Copyright 2018, Springer Nature. c) Cross-sectional schematic structure of an ionic skin pressure sensor device (top), and relative capacitance changes of the pressure sensor array responding to two 20 g weights (bottom). Reproduced with permission.[176] Copyright 2019, Royal Society of Chemistry.

sensor in a stretchable format using a gel electrolyte.[176] A gelatin based, deep eutectic solvent gel electrolyte was used to suppress the volatility of the solvent (Figure 12c). The fabricated capacitive pressure sensor maintained a linear response in the range of 0–16 kPa and pressure sensitivity as low as 1 kPa.

Strain sensors are commonly used physical sensors. A highly sensitive and stretchable resistive strain sensor from fully rubbery materials was demonstrated by Kim et al.[60] The rubbery semiconductor, P3HT-NFs percolated in PDMS, was used as the highly stretchable sensing element with AgNWs embedded in PDMS as the two terminal electrodes. The fabricated strain sensor had a high gauge factor of 32 with a good strain response under mechanical stretching up to 100%. To demonstrate its applicability, a smart glove with rubbery strain sensors was constructed for strain mapping during hand motions (**Figure 13**a). Other types of strain sensors have also been examined. Xu et al. fabricated a highly sensitive biocompatible capacitive strain sensor using an ionic nanocomposite as the sensing element (Figure 13b).[184] The ionic nanocomposite was prepared with ionic hydrogel and silver nanofibers (AgNFs). The sensor had an ultrahigh stretchability of 1000% and a high gauge factor of 165. The addition of AgNFs into the hydrogel induced an enlarged EDL at the interface between the hydrogel and metal, which caused around three orders of strain sensitivity. The fabricated sensors were used for various types of physiological signal monitoring, including arm and finger motions, pulse, electrocardiography (ECG), breathing, speaking, and facial expressions.

Rubbery temperature sensors have also found interesting applications. Trung et al. composed a transparent and stretchable temperature sensor based on a rubber-like transistor.[188] The composite based on reduced graphene oxide (rGO) NSs in elastomeric PU was used as both the sensing and semiconductor layers (**Figure 14**a). A PEDOT:PSS/PU composite and PU were used for the electrodes and gate dielectric, respectively. The fabricated sensor showed a high sensitivity of ≈1.34% per °C with a high mechanical stretchability of 70%. The responsivity of the sensor was maintained after 10 000 cycles of 30% stretching. A 4 × 4 array sufficiently mapped the temperature distribution of various body parts. As an example of an organic semiconductor based rubbery temperature sensor, Kim et al. used a rubbery P3HT-NFs/PDMS semiconductor based two terminal temperature sensor with AgNW embedded in PDMS.[59] The resistance of the sensor demonstrated good temperature dependency from 30 to 50 °C (Figure 14b). A robot hand with the temperature sensor was contacted to a cup containing hot and cold water to highlight the response of the temperature sensor.

Various other types of rubbery sensors, such as chemical sensors, humidity sensors, etc. have also been reported. Jin et al. developed an ultrastable chemiresistor sensor from a rubber-like stretchable component and an intrinsically stretchable polymer electrolyte (**Figure 15**a).[190] A thermoplastic PU matrix and EMIM-TFSI ionic liquid were used to form a solid-state polymer electrolyte. Different molecular interactions between the polymer electrolyte and volatile organic compound caused ionic conductivity changes in the polymer electrolyte. The sensor showed a clear resistance change under chemical environments with five different volatile organic compounds, including toluene, hexane, propanol, ethanol, and acetone. In addition, the devices presented a low limit of detection of ≈1 ppm with a sensitivity of 1.6% for toluene and operated reliably under harsh environmental conditions (relative humidity, RH, of 85% or temperature of 100 °C) as well as mechanical deformations such as bending (bending to a radius of curvature of 1 mm) and stretching (strain of 100%). The rubbery humidity

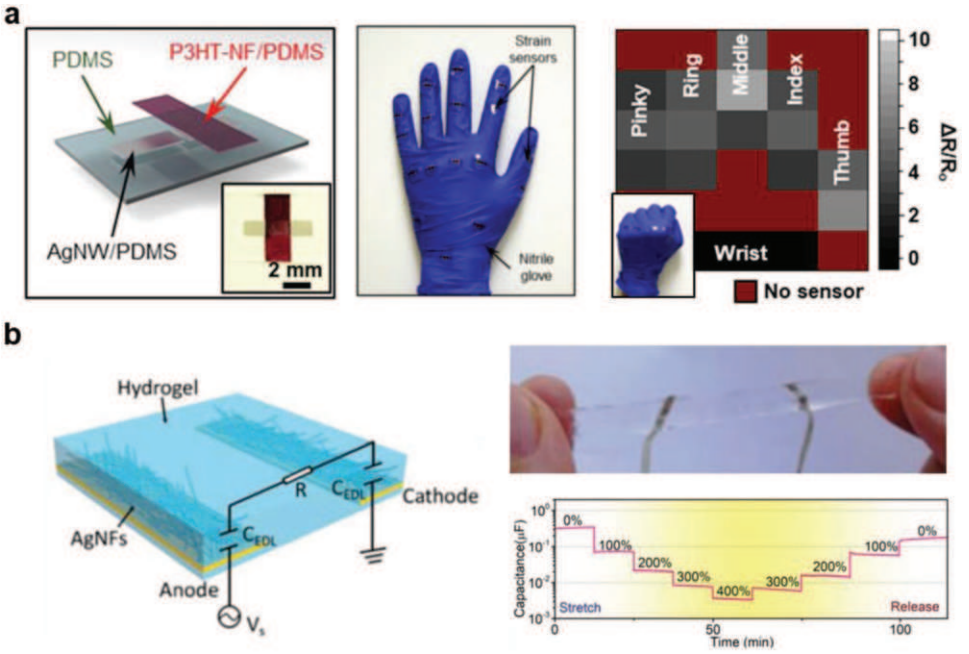

Figure 13. Rubbery strain sensors. a) Exploded schematic illustration of the rubbery strain sensor. Inset is the photograph of the strain sensor (left), photograph of a glove with the rubbery strain sensors (middle), and mapping the normalized electrical resistance change ($\Delta R/R_o$) of the strain sensors under the clenched fist motion (right). Reproduced with permission.[60] Copyright 2018, American Chemical Society. b) Structural schematic of the capacitive-type strain sensor based on the hydrogel-AgNF nanocomposite (left), photograph of the b-hydrogel strain sensor showing excellent stretchability (right, top), and time-dependent capacitance of the b-hydrogel strain sensor (right, bottom). Reproduced with permission.[184] Copyright 2019, Royal Society of Chemistry.

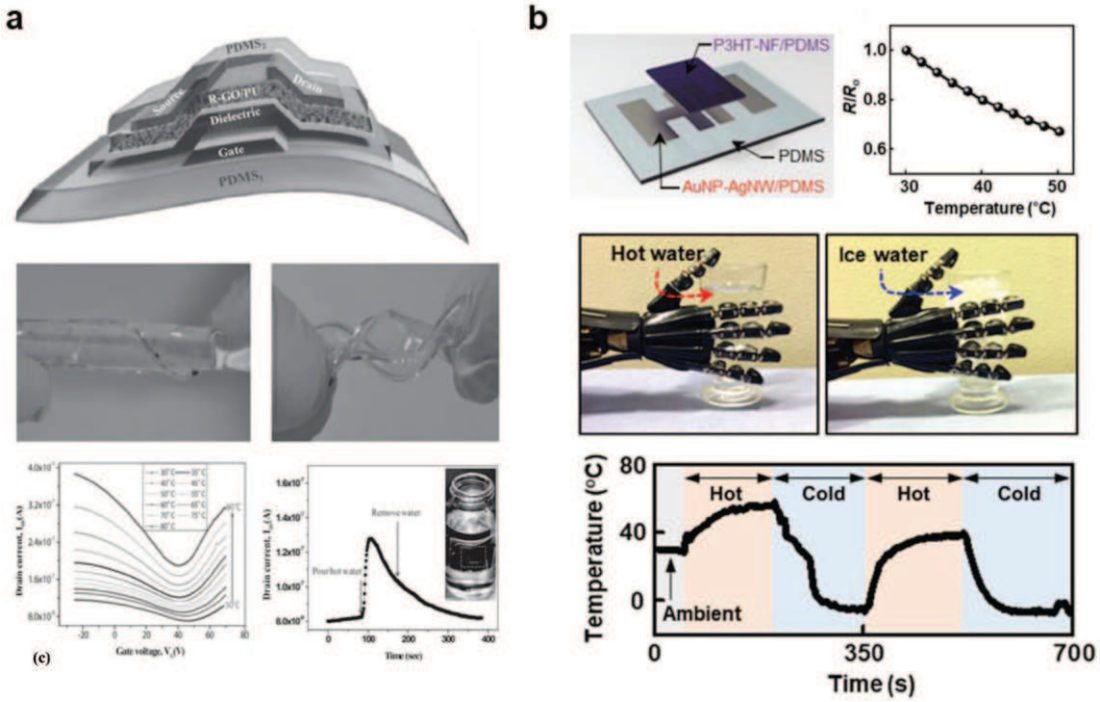

Figure 14. Rubbery temperature sensors. a) Schematic of the transparent and stretchable gated temperature sensor (top), optical images of device under mechanical deformation (middle), transfer characteristics of the device measured over different temperatures (bottom, left), and current responses of the sensor to hot water (bottom, right) Reproduced with permission.[188] Copyright 2015, Wiley-VCH. b) Exploded schematic illustration of the temperature sensor (top, left), relative electrical resistance change of the temperature sensor with respect to the different temperatures (top, right), photographs of the robotic hand with the temperature sensor touching hot (middle, left) and cold (middle, right) cups, and measured sensor responses while the hand with artificial skin touched the hot and cold cups alternatively (bottom). Reproduced under the terms and conditions of the CC-BY-NC Creative Commons Attribution NonCommercial License 4.0.[59] Copyright 2017, The Authors, published by the American Association for the Advancement of Science.

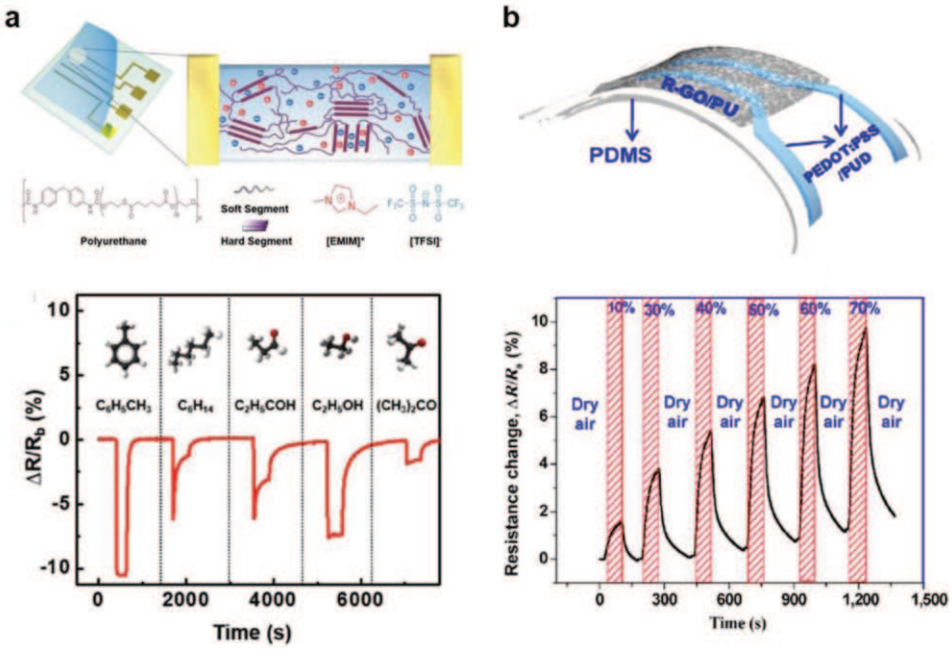

Figure 15. Rubbery chemiresistors and humidity sensors. a) Schematic illustration of the ionic chemiresistor skin based on TPU polymer matrix with ionic liquid [EMIM][TFSI] (top) and dynamic sensing behavior of the device to various target volatile organic compounds, including toluene, hexane, propanol, ethanol, and acetone (bottom). Reproduced with permission.[190] Copyright 2018, Wiley-VCH. b) Schematic of the transparent, stretchable humidity sensor (top) and resistance changes in the transparent, stretchable humidity sensor when the humidity was gradually increased (from 10% to 70%) (bottom). Reproduced with permission.[191] Copyright 2017, Springer Nature.

sensor is also an emerging device.[191,192] Trung et al. developed a transparent, stretchable humidity sensor from a rubber-like stretchable component.[191] An rGO-PU composite was used as the rubbery sensing element and PEDOT:PSS/PU was used as the elastomeric conductor (Figure 15b). The humidity sensor showed fast response of 3.5 s and relaxation time of 7 s, and its sensing capability was almost unchanged under a mechanical strain of 60% and after 10 000 stretching cycles at 40% strain.

6. Conclusion and Outlook

In this review, we have summarized the latest major advances in intrinsically stretchable rubbery electronic materials, including conductors, semiconductors, and dielectrics. These rubbery electronic materials, organized and assembled rationally, have led to the realization of rubbery electronics, including various active electronics and sensors. Constructing stretchable electronics all from rubbery electronic materials is a new technical pathway for stretchable electronics and electronics in general. Compared with stretchable electronics based on nonstretchable materials, rubbery electronics offer many distinct advantages owing to their physical nature and mechanical features. For instance, rubbery electronics could be naturally integrated with soft biological systems, such as organs, tissues, in a seamless manner.[65,169,193] Although their development is relatively new, rubbery electronics have already shown their promising usages in many fields, such as biomedical,[184,188,193,196] wearable,[169,175,193] robotics,[59,133] etc.

Although rubbery transistors,[41,52,59,64,65,133,169] optoelectronics,[64,99,170–174] and sensors[59,60,169,175–189] have been conceived, to realize these rubbery devices with high performances is still challenging. For instance, the carrier mobilities of the rubbery semiconductors and the conductivity of rubbery conductors are both relatively low, the individual device size is relatively large and the integration density is low, and the parasitic effects are still significant. These collectively lead to their relatively low performances to achieve many important electrical functions, such as switching, amplifying, etc. Although enormous potential exists, rubbery electronics and their associated device technologies are far from mature and even immediate commercialization due to several challenges such as reliable materials, scalable manufacturing, and performance uniformity and stability. The future development of rubbery electronics may directly address these challenges. For instance, how to design and manufacture high performance rubbery electronic materials, such as conductors and semiconductors in various formats, and a comprehensive understanding of their structure–property relationships are needed through detailed experimental and theoretical investigation. In addition to the materials aspect, reliable device fabrication, assembly, and packaging technologies in a scalable manner are needed to promote rubbery electronics to reach their broad applications. Since much effort has and will be made continuously, we expect to see more advances in rubbery electronics from different aspects to come in the near future.

Acknowledgements

C.Y. would like to thank the National Science Foundation CAREER grant (CMMI-1554499), the Doctoral New Investigator grant from American Chemical Society Petroleum Research Fund (56840-DNI7), the Office of Naval Research grant (N00014-18-1-2338) under Young Investigator Program and 3M non-tenured faculty award.

Conflict of Interest

The authors declare no conflict of interest.

Keywords

elastomeric electronic materials, rubbery conductors, rubbery electronics, rubbery semiconductors, stretchable electronics

Received: April 16, 2019
Revised: May 10, 2019
Published online:

[1] A. Koh, D. Kang, Y. Xue, S. Lee, R. M. Pielak, J. Kim, T. Hwang, S. Min, A. Banks, P. Bastien, *Sci. Transl. Med.* **2016**, *8*, 366ra165.
[2] T. Yokota, P. Zalar, M. Kaltenbrunner, H. Jinno, N. Matsuhisa, H. Kitanosako, Y. Tachibana, W. Yukita, M. Koizumi, T. Someya, *Sci. Adv.* **2016**, *2*, e1501856.
[3] I. l. Agua, D. Mantione, U. Ismailov, A. Sanchez-Sanchez, N. Aramburu, G. G. Malliaras, D. Mecerreyes, E. Ismailova, *Adv. Mater. Technol.* **2018**, *3*, 1700322.
[4] Y. Liu, M. Pharr, G. A. Salvatore, *ACS Nano* **2017**, *11*, 9614.
[5] S. Choi, S. I. Han, D. Jung, H. J. Hwang, C. Lim, S. Bae, O. K. Park, C. M. Tschabrunn, M. Lee, S. Y. Bae, J. W. Yu, J. H. Ryu, S.-W. Lee, K. Park, P. M. Kang, W. B. Lee, R. Nezafat, T. Hyeon, D.-H. Kim, *Nat. Nanotechnol.* **2018**, *13*, 1048.
[6] S. Gong, W. Cheng, *Adv. Energy Mater.* **2017**, *7*, 1700648.
[7] D.-H. Kim, R. Ghaffari, N. Lu, S. Wang, S. P. Lee, H. Keum, R. D'Angelo, L. Klinker, Y. Su, C. Lu, Y.-S. Kim, A. Ameen, Y. Li, Y. Zhang, B. de Graff, Y.-Y. Hsu, Z. Liu, J. Ruskin, L. Xu, C. Lu, F. G. Omenetto, Y. Huang, M. Mansour, M. J. Slepian, J. A. Rogers, *Proc. Natl. Acad. Sci. U S A* **2012**, *109*, 19910.
[8] L. Li, H. Xiang, Y. Xiong, H. Zhao, Y. Bai, S. Wang, F. Sun, M. Hao, L. Liu, T. Li, Z. Peng, J. Xu, T. Zhang, *Adv. Sci.* **2018**, *5*, 1800558.
[9] M. A. Parvez Mahmud, N. Huda, S. H. Farjana, M. Asadnia, C. Lang, *Adv. Energy Mater.* **2018**, *8*, 1701210.
[10] L. Xu, S. R. Gutbrod, A. P. Bonifas, Y. Su, M. S. Sulkin, N. Lu, H.-J. Chung, K.-I. Jang, Z. Liu, M. Ying, C. Lu, R. C. Webb, J.-S. Kim, J. I. Laughner, H. Cheng, Y. Liu, A. Ameen, J.-W. Jeong, G.-T. Kim, Y. Huang, I. R. Efimov, J. A. Rogers, *Nat. Commun.* **2014**, *5*, 3329.
[11] J. Kim, G. A. Salvatore, H. Araki, A. M. Chiarelli, Z. Xie, A. Banks, X. Sheng, Y. Liu, J. W. Lee, K.-I. Jang, *Sci. Adv.* **2016**, *2*, e1600418.
[12] A. Chortos, J. Liu, Z. Bao, *Nat. Mater.* **2016**, *15*, 937.
[13] J. Ge, L. Sun, F.-R. Zhang, Y. Zhang, L.-A. Shi, H.-Y. Zhao, H.-W. Zhu, H.-L. Jiang, S.-H. Yu, *Adv. Mater.* **2016**, *28*, 722.
[14] S. Han, M. K. Kim, B. Wang, D. S. Wie, S. Wang, C. H. Lee, *Adv. Mater.* **2016**, *28*, 10257.
[15] Y. Song, W. Huang, C. Mu, X. Chen, Q. Zhang, A. Ran, Z. Peng, R. Sun, W. Xie, *Adv. Mater. Technol.* **2019**, *4*, 1800680.
[16] Y. Guo, M. Zhong, Z. Fang, P. Wan, G. Yu, *Nano Lett.* **2019**, *19*, 1143.
[17] X. Liao, W. Song, X. Zhang, H. Huang, Y. Wang, Y. Zheng, *J. Mater. Chem. C* **2018**, *6*, 12841.
[18] Y. Liu, J. J. S. Norton, R. Qazi, Z. Zou, K. R. Ammann, H. Liu, L. Yan, P. L. Tran, K.-I. Jang, J. W. Lee, D. Zhang, K. A. Kilian, S. H. Jung, T. Bretl, J. Xiao, M. J. Slepian, Y. Huang, J.-W. Jeong, J. A. Rogers, *Sci. Adv.* **2016**, *2*, e1601185.
[19] H. Wang, X. Ma, Y. Hao, *Adv. Mater. Interfaces* **2017**, *4*, 1600709.
[20] J. Wang, M.-F. Lin, S. Park, P. S. Lee, *Mater. Today* **2018**, *21*, 508.
[21] H. Chen, L. Bai, T. Li, C. Zhao, J. Zhang, N. Zhang, G. Song, Q. Gan, Y. Xu, *Nano Energy* **2018**, *46*, 73.
[22] A. Kumar, *Manuf. Lett.* **2018**, *15*, 122.
[23] J. Park, J. Kim, K. Kim, S.-Y. Kim, W. H. Cheong, K. Park, J. H. Song, G. Namgoong, J. J. Kim, J. Heo, F. Bien, J.-U. Park, *Nanoscale* **2016**, *8*, 10591.
[24] M. Swan, *J. Sens. Actuator Networks* **2012**, *1*, 217.
[25] M. Kaltenbrunner, T. Sekitani, J. Reeder, T. Yokota, K. Kuribara, T. Tokuhara, M. Drack, R. Schwodiauer, I. Graz, S. Bauer-Gogonea, S. Bauer, T. Someya, *Nature* **2013**, *499*, 458.
[26] Y. Sun, W. M. Choi, H. Jiang, Y. Y. Huang, J. A. Rogers, *Nat. Nanotechnol.* **2006**, *1*, 201.
[27] J. Kim, M. Lee, H. J. Shim, R. Ghaffari, H. R. Cho, D. Son, Y. H. Jung, M. Soh, C. Choi, S. Jung, K. Chu, D. Jeon, S.-T. Lee, J. H. Kim, S. H. Choi, T. Hyeon, D.-H. Kim, *Nat. Commun.* **2014**, *5*, 5747.
[28] C. Dagdeviren, Y. Shi, P. Joe, R. Ghaffari, G. Balooch, K. Usgaonkar, O. Gur, P. L. Tran, J. R. Crosby, M. Meyer, *Nat. Mater.* **2015**, *14*, 728.
[29] J. Kim, A. Banks, H. Cheng, Z. Xie, S. Xu, K.-I. Jang, J. W. Lee, Z. Liu, P. Gutruf, X. Huang, P. Wei, F. Liu, K. Li, M. Dalal, R. Ghaffari, X. Feng, Y. Huang, S. Gupta, U. Paik, J. A. Rogers, *Small* **2015**, *11*, 906.
[30] S. Xu, Y. Zhang, J. Cho, J. Lee, X. Huang, L. Jia, J. A. Fan, Y. Su, J. Su, H. Zhang, H. Cheng, B. Lu, C. Yu, C. Chuang, T.-i. Kim, T. Song, K. Shigeta, S. Kang, C. Dagdeviren, I. Petrov, P. V. Braun, Y. Huang, U. Paik, J. A. Rogers, *Nat. Commun.* **2013**, *4*, 1543.
[31] S.-I. Park, Y. Xiong, R.-H. Kim, P. Elvikis, M. Meitl, D.-H. Kim, J. Wu, J. Yoon, C.-J. Yu, Z. Liu, Y. Huang, K.-c. Hwang, P. Ferreira, X. Li, K. Choquette, J. A. Rogers, *Science* **2009**, *325*, 977.
[32] M. Isobe, K. Okumura, *Sci. Rep.* **2016**, *6*, 24758.
[33] A. Lamoureux, K. Lee, M. Shlian, S. R. Forrest, M. Shtein, *Nat. Commun.* **2015**, *6*, 8092.
[34] T. C. Shyu, P. F. Damasceno, P. M. Dodd, A. Lamoureux, L. Xu, M. Shlian, M. Shtein, S. C. Glotzer, N. A. Kotov, *Nat. Mater.* **2015**, *14*, 785.
[35] M. Shin, J. Y. Oh, K. E. Byun, Y. J. Lee, B. Kim, H. K. Baik, J. J. Park, U. Jeong, *Adv. Mater.* **2015**, *27*, 1255.
[36] J. Liang, L. Li, D. Chen, T. Hajagos, Z. Ren, S. Y. Chou, W. Hu, Q. Pei, *Nat. Commun.* **2015**, *6*, 7647.
[37] T. Higashihara, S. Fukuta, Y. Ochiai, T. Sekine, K. Chino, T. Koganezawa, I. Osaka, *ACS Appl. Polym. Mater.* **2019**, *1*, 315.
[38] C. Lu, W.-Y. Lee, X. Gu, J. Xu, H.-H. Chou, H. Yan, Y.-C. Chiu, M. He, J. R. Matthews, W. Niu, J. B.-H. Tok, M. F. Toney, W.-C. Chen, Z. Bao, *Adv. Electron. Mater.* **2017**, *3*, 1600311.
[39] C. Müller, S. Goffri, D. W. Breiby, J. W. Andreasen, H. D. Chanzy, R. A. J. Janssen, M. M. Nielsen, C. P. Radano, H. Sirringhaus, P. Smith, N. Stingelin-Stutzmann, *Adv. Funct. Mater.* **2007**, *17*, 2674.
[40] J. Mun, G.-J. N. Wang, J. Y. Oh, T. Katsumata, F. L. Lee, J. Kang, H.-C. Wu, F. Lissel, S. Rondeau-Gagné, J. B.-H. Tok, Z. Bao, *Adv. Funct. Mater.* **2018**, *28*, 1804222.
[41] J. Y. Oh, S. Rondeau-Gagné, Y.-C. Chiu, A. Chortos, F. Lissel, G.-J. N. Wang, B. C. Schroeder, T. Kurosawa, J. Lopez, T. Katsumata, J. Xu, C. Zhu, X. Gu, W.-G. Bae, Y. Kim, L. Jin, J. W. Chung, J. B. H. Tok, Z. Bao, *Nature* **2016**, *539*, 411.
[42] R. Peng, B. Pang, D. Hu, M. Chen, G. Zhang, X. Wang, H. Lu, K. Cho, L. Qiu, *J. Mater. Chem. C* **2015**, *3*, 3599.
[43] S. Savagatrup, A. D. Printz, D. Rodriquez, D. J. Lipomi, *Macromolecules* **2014**, *47*, 1981.
[44] S. Savagatrup, X. Zhao, E. Chan, J. Mei, D. J. Lipomi, *Macromol. Rapid Commun.* **2016**, *37*, 1623.
[45] S. Y. Son, J.-H. Kim, E. Song, K. Choi, J. Lee, K. Cho, T.-S. Kim, T. Park, *Macromolecules* **2018**, *51*, 2572.
[46] S. Savagatrup, A. S. Makaram, D. J. Burke, D. J. Lipomi, *Adv. Funct. Mater.* **2014**, *24*, 1169.

[47] S. Savagatrup, A. D. Printz, H. Wu, K. M. Rajan, E. J. Sawyer, A. V. Zaretski, C. J. Bettinger, D. J. Lipomi, *Synth. Met.* **2015**, *203*, 208.
[48] Z. C. Smith, Z. M. Wright, A. M. Arnold, G. Sauvé, R. D. McCullough, S. A. Sydlik, *Adv. Electron. Mater.* **2017**, *3*, 1600316.
[49] H.-F. Wen, H.-C. Wu, J. Aimi, C.-C. Hung, Y.-C. Chiang, C.-C. Kuo, W.-C. Chen, *Macromolecules* **2017**, *50*, 4982.
[50] H.-C. Wu, C.-C. Hung, C.-W. Hong, H.-S. Sun, J.-T. Wang, G. Yamashita, T. Higashihara, W.-C. Chen, *Macromolecules* **2016**, *49*, 8540.
[51] P.-H. Chu, G. Wang, B. Fu, D. Choi, J. O. Park, M. Srinivasarao, E. Reichmanis, *Adv. Electron. Mater.* **2016**, *2*, 1500384.
[52] J. I. Scott, X. Xue, M. Wang, R. J. Kline, B. C. Hoffman, D. Dougherty, C. Zhou, G. Bazan, B. T. O'Connor, *ACS Appl. Mater. Interfaces* **2016**, *8*, 14037.
[53] T. Sun, J. I. Scott, M. Wang, R. J. Kline, G. C. Bazan, B. T. O'Connor, *Adv. Electron. Mater.* **2017**, *3*, 1600388.
[54] B. O'Connor, R. J. Kline, B. R. Conrad, L. J. Richter, D. Gundlach, M. F. Toney, D. M. DeLongchamp, *Adv. Funct. Mater.* **2011**, *21*, 3697.
[55] M. Chang, Z. Su, E. Egap, *Macromolecules* **2016**, *49*, 9449.
[56] Y.-C. Chiang, C.-C. Shih, S.-H. Tung, W.-C. Chen, *Polymer* **2018**, *155*, 146.
[57] S. Goffri, C. Müller, N. Stingelin-Stutzmann, D. W. Breiby, C. P. Radano, J. W. Andreasen, R. Thompson, R. A. J. Janssen, M. M. Nielsen, P. Smith, H. Sirringhaus, *Nat. Mater.* **2006**, *5*, 950.
[58] H.-C. Hsieh, J.-Y. Chen, W.-Y. Lee, D. Bera, W.-C. Chen, *Macromol. Rapid Commun.* **2018**, *39*, 1700616.
[59] H.-J. Kim, K. Sim, A. Thukral, C. Yu, *Sci. Adv.* **2017**, *3*, e1701114.
[60] H.-J. Kim, A. Thukral, C. Yu, *ACS Appl. Mater. Interfaces* **2018**, *10*, 5000.
[61] J. Moulton, P. Smith, *J. Polym. Sci., Part B: Polym. Phys.* **1992**, *30*, 871.
[62] L. Qiu, X. Wang, W. H. Lee, J. A. Lim, J. S. Kim, D. Kwak, K. Cho, *Chem. Mater.* **2009**, *21*, 4380.
[63] M. Shin, J. Y. Oh, K.-E. Byun, Y.-J. Lee, B. Kim, H.-K. Baik, J.-J. Park, U. Jeong, *Adv. Mater.* **2015**, *27*, 1255.
[64] K. Sim, Z. Rao, H.-J. Kim, A. Thukral, H. Shim, C. Yu, *Sci. Adv.* **2019**, *5*, eaav5749.
[65] J. Xu, S. Wang, G.-J. N. Wang, C. Zhu, S. Luo, L. Jin, X. Gu, S. Chen, V. R. Feig, J. W. F. To, S. Rondeau-Gagné, J. Park, B. C. Schroeder, C. Lu, J. Y. Oh, Y. Wang, Y.-H. Kim, H. Yan, R. Sinclair, D. Zhou, G. Xue, B. Murmann, C. Linder, W. Cai, J. B.-H. Tok, J. W. Chung, Z. Bao, *Science* **2017**, *355*, 59.
[66] E. Song, B. Kang, H. H. Choi, D. H. Sin, H. Lee, W. H. Lee, K. Cho, *Adv. Electron. Mater.* **2016**, *2*, 1500250.
[67] L. Qiu, J. A. Lim, X. Wang, W. H. Lee, M. Hwang, K. Cho, *Adv. Mater.* **2008**, *20*, 1141.
[68] S. Wang, S. Fabiano, S. Himmelberger, S. Puzinas, X. Crispin, A. Salleo, M. Berggren, *Proc. Natl. Acad. Sci. U S A* **2015**, *112*, 10599.
[69] G. Zhang, M. McBride, N. Persson, S. Lee, T. J. Dunn, M. F. Toney, Z. Yuan, Y.-H. Kwon, P.-H. Chu, B. Risteen, E. Reichmanis, *Chem. Mater.* **2017**, *29*, 7645.
[70] M. Y. Teo, N. Kim, S. Kee, B. S. Kim, G. Kim, S. Hong, S. Jung, K. Lee, *ACS Appl. Mater. Interfaces* **2017**, *9*, 819.
[71] Y. Wang, C. Zhu, R. Pfattner, H. Yan, L. Jin, S. Chen, F. Molina-Lopez, F. Lissel, J. Liu, N. I. Rabiah, Z. Chen, J. W. Chung, C. Linder, M. F. Toney, B. Murmann, Z. Bao, *Sci. Adv.* **2017**, *3*, e1602076.
[72] S. W. Jin, J. Park, S. Y. Hong, H. Park, Y. R. Jeong, J. Park, S. S. Lee, J. S. Ha, *Sci. Rep.* **2015**, *5*, 11695.
[73] A. Patra, M. Bendikov, S. Chand, *Acc. Chem. Res.* **2014**, *47*, 1465.
[74] P. Baek, L. Voorhaar, D. Barker, J. Travas-Sejdic, *Acc. Chem. Res.* **2018**, *51*, 1581.
[75] H. Shi, C. C. Liu, Q. L. Jiang, J. K. Xu, *Adv. Electron. Mater.* **2015**, *1*, 1500017.
[76] J. Y. Oh, S. Kim, H. K. Baik, U. Jeong, *Adv. Mater.* **2016**, *28*, 4455.
[77] S. Zhang, E. Hubis, G. Tomasello, G. Soliveri, P. Kumar, F. Cicoira, *Chem. Mater.* **2017**, *29*, 3126.
[78] J.-S. Noh, *RSC Adv.* **2014**, *4*, 1857.
[79] Y.-F. Liu, J. Feng, Y.-G. Bi, D. Yin, H.-B. Sun, *Adv. Mater. Technol.* **2019**, *4*, 1800371.
[80] S. Savagatrup, E. Chan, S. M. Renteria-Garcia, A. D. Printz, A. V. Zaretski, T. F. O'Connor, D. Rodriquez, E. Valle, D. J. Lipomi, *Adv. Funct. Mater.* **2015**, *25*, 427.
[81] B. Xu, J. Hou, *Adv. Energy Mater.* **2018**, *8*, 1800022.
[82] B. Lu, H. Yuk, S. Lin, N. Jian, K. Qu, J. Xu, X. Zhao, *Nat. Commun.* **2019**, *10*, 1043.
[83] J. Y. Ouyang, *Acta Phys-Chim. Sin.* **2018**, *34*, 1211.
[84] R. Balint, N. J. Cassidy, S. H. Cartmell, *Acta Biomater.* **2014**, *10*, 2341.
[85] Y. Liu, K. Ai, L. Lu, *Chem. Rev.* **2014**, *114*, 5057.
[86] N. Kim, S. Kee, S. H. Lee, B. H. Lee, Y. H. Kahng, Y. R. Jo, B. J. Kim, K. Lee, *Adv. Mater.* **2014**, *26*, 2268.
[87] R. Singh, J. Tharion, S. Murugan, A. Kumar, *ACS Appl. Mater. Interfaces* **2017**, *9*, 19427.
[88] K. Nagamine, S. Chihara, H. Kai, H. Kaji, M. Nishizawa, *Sens. Actuators, B.* **2016**, *237*, 49.
[89] X. Strakosas, B. Wei, D. C. Martin, R. M. Owens, *J. Mater. Chem. B* **2016**, *4*, 4952.
[90] Z. Wen, Y. Yang, N. Sun, G. Li, Y. Liu, C. Chen, J. Shi, L. Xie, H. Jiang, D. Bao, Q. Zhuo, X. Sun, *Adv. Funct. Mater.* **2018**, *28*, 1803684.
[91] D. Alemu Mengistie, P.-C. Wang, C.-W. Chu, *J. Mater. Chem. A* **2013**, *1*, 9907.
[92] A. de Izarra, S. Park, J. Lee, Y. Lansac, Y. H. Jang, *J. Am. Chem. Soc.* **2018**, *140*, 5375.
[93] J. H. Lee, Y. R. Jeong, G. Lee, S. W. Jin, Y. H. Lee, S. Y. Hong, H. Park, J. W. Kim, S.-S. Lee, J. S. Ha, *ACS Appl. Mater. Interfaces* **2018**, *10*, 28027.
[94] C. M. Palumbiny, F. Liu, T. P. Russell, A. Hexemer, C. Wang, P. Muller-Buschbaum, *Adv. Mater.* **2015**, *27*, 3391.
[95] M. Vosgueritchian, D. J. Lipomi, Z. Bao, *Adv. Funct. Mater.* **2012**, *22*, 421.
[96] M. Park, J. Im, M. Shin, Y. Min, J. Park, H. Cho, S. Park, M.-B. Shim, S. Jeon, D.-Y. Chung, J. Bae, J. Park, U. Jeong, K. Kim, *Nat. Nanotechnol.* **2012**, *7*, 803.
[97] N. Matsuhisa, D. Inoue, P. Zalar, H. Jin, Y. Matsuba, A. Itoh, T. Yokota, D. Hashizume, T. Someya, *Nat. Mater.* **2017**, *16*, 834.
[98] K. Y. Chun, Y. Oh, J. Rho, J. H. Ahn, Y. J. Kim, H. R. Choi, S. Baik, *Nat. Nanotechnol.* **2010**, *5*, 853.
[99] J. Liang, L. Li, X. Niu, Z. Yu, Q. Pei, *Nat. Photonics* **2013**, *7*, 817.
[100] S. Gong, W. L. Cheng, *Adv. Electron. Mater.* **2017**, *3*, 1600314.
[101] M. Park, J. Park, U. Jeong, *Nano Today* **2014**, *9*, 244.
[102] C. Wang, C. Wang, Z. Huang, S. Xu, *Adv. Mater.* **2018**, *30*, 1801368.
[103] S. S. Yao, Y. Zhu, *Adv. Mater.* **2015**, *27*, 1480.
[104] T. Sekitani, Y. Noguchi, K. Hata, T. Fukushima, T. Aida, T. Someya, *Science* **2008**, *321*, 1468.
[105] G. E. Pike, C. H. Seager, *Phys. Rev. B* **1974**, *10*, 1421.
[106] S. Kirkpatrick, *Rev. Mod. Phys.* **1973**, *45*, 574.
[107] F. He, S. Lau, H. L. Chan, J. Fan, *Adv. Mater.* **2009**, *21*, 710.
[108] M. Panda, V. Srinivas, A. K. Thakur, *Appl. Phys. Lett.* **2008**, *92*, 132905.
[109] J. Li, J.-K. Kim, *Compos. Sci. Technol.* **2007**, *67*, 2114.
[110] Y. Kim, J. Zhu, B. Yeom, M. Di Prima, X. Su, J. G. Kim, S. J. Yoo, C. Uher, N. A. Kotov, *Nature* **2013**, *500*, 59.
[111] S. Zhu, J.-H. So, R. Mays, S. Desai, W. R. Barnes, B. Pourdeyhimi, M. D. Dickey, *Adv. Funct. Mater.* **2013**, *23*, 2308.
[112] Y. Yang, S. Ding, T. Araki, J. T. Jiu, T. Sugahara, J. Wang, J. Vanfleteren, T. Sekitani, K. Suganuma, *Nano Res.* **2016**, *9*, 401.

[113] J. Liu, W.-Q. Cao, H.-B. Jin, J. Yuan, D.-Q. Zhang, M.-S. Cao, *J. Mater. Chem. C* **2015**, *3*, 4670.
[114] B. W. Zhu, S. Gong, F. G. Lin, Y. Wang, Y. Z. Ling, T. C. An, W. L. Cheng, *Adv. Electron. Mater.* **2019**, *5*, 1800509.
[115] X. Wang, T. Li, J. Adams, J. Yang, *J. Mater. Chem. A* **2013**, *1*, 3580.
[116] S. Cho, J. H. Song, M. Kong, S. Shin, Y. T. Kim, G. Park, C. G. Park, T. J. Shin, J. Myoung, U. Jeong, *ACS Appl. Mater. Interfaces* **2017**, *9*, 44096.
[117] N. Matsuhisa, M. Kaltenbrunner, T. Yokota, H. Jinno, K. Kuribara, T. Sekitani, T. Someya, *Nat. Commun.* **2015**, *6*, 7461.
[118] R. Ma, S.-Y. Chou, Y. Xie, Q. Pei, *Chem. Soc. Rev.* **2019**, *48*, 1741.
[119] J. Zhao, Z. Chi, Z. Yang, X. Chen, M. S. Arnold, Y. Zhang, J. Xu, Z. Chi, M. P. Aldred, *Nanoscale* **2018**, *10*, 5764.
[120] C. M. Stafford, C. Harrison, K. L. Beers, A. Karim, E. J. Amis, M. R. VanLandingham, H.-C. Kim, W. Volksen, R. D. Miller, E. E. Simonyi, *Nat. Mater.* **2004**, *3*, 545.
[121] H. Wu, S. Kustra, E. M. Gates, C. J. Bettinger, *Org. Electron.* **2013**, *14*, 1636.
[122] D. J. Lipomi, B. C.-K. Tee, M. Vosgueritchian, Z. Bao, *Adv. Mater.* **2011**, *23*, 1771.
[123] M. Kaltenbrunner, M. S. White, E. D. Głowacki, T. Sekitani, T. Someya, N. S. Sariciftci, S. Bauer, *Nat. Commun.* **2012**, *3*, 770.
[124] P. Z. Hanakata, Z. Qi, D. K. Campbell, H. S. Park, *Nanoscale* **2016**, *8*, 458.
[125] M. K. Blees, A. W. Barnard, P. A. Rose, S. P. Roberts, K. L. McGill, P. Y. Huang, A. R. Ruyack, J. W. Kevek, B. Kobrin, D. A. Muller, P. L. McEuen, *Nature* **2015**, *524*, 204.
[126] M. Amjadi, M. Turan, C. P. Clementson, M. Sitti, *ACS Appl. Mater. Interfaces* **2016**, *8*, 5618.
[127] A. Chortos, J. Lim, J. W. F. To, M. Vosgueritchian, T. J. Dusseault, T.-H. Kim, S. Hwang, Z. Bao, *Adv. Mater.* **2014**, *26*, 4253.
[128] M. U. Ocheje, B. P. Charron, A. Nyayachavadi, S. Rondeau-Gagné, *Flexible and Printed Electron.* **2017**, *2*, 043002.
[129] M. A. Alkhadra, S. E. Root, K. M. Hilby, D. Rodriquez, F. Sugiyama, D. J. Lipomi, *Chem. Mater.* **2017**, *29*, 10139.
[130] F. Sugiyama, A. T. Kleinschmidt, L. V. Kayser, D. Rodriquez, M. Finn, M. A. Alkhadra, J. M. H. Wan, J. Ramírez, A. S. C. Chiang, S. E. Root, S. Savagatrup, D. J. Lipomi, *Polym. Chem.* **2018**, *9*, 4354.
[131] D. Rodriquez, J.-H. Kim, S. E. Root, Z. Fei, P. Boufflet, M. Heeney, T.-S. Kim, D. J. Lipomi, *ACS Appl. Mater. Interfaces* **2017**, *9*, 8855.
[132] A. T. Kleinschmidt, D. J. Lipomi, *Acc. Chem. Res.* **2018**, *51*, 3134.
[133] H.-J. Kim, A. Thukral, S. Sharma, C. Yu, *Adv. Mater. Technol.* **2018**, *3*, 1800043.
[134] S. H. Chae, W. J. Yu, J. J. Bae, D. L. Duong, D. Perello, H. Y. Jeong, Q. H. Ta, T. H. Ly, Q. A. Vu, M. Yun, X. Duan, Y. H. Lee, *Nat. Mater.* **2013**, *12*, 403.
[135] R. Raveendran, M. A. G. Namboothiry, *ACS Omega* **2018**, *3*, 11278.
[136] M.-m. Ling, Z. Bao, D. Li, *Appl. Phys. Lett.* **2006**, *88*, 033502.
[137] C. Reese, W.-J. Chung, M.-m. Ling, M. Roberts, Z. Bao, *Appl. Phys. Lett.* **2006**, *89*, 202108.
[138] J. Shi, M. B. Chan-Park, C. M. Li, *ACS Appl. Mater. Interfaces* **2011**, *3*, 1880.
[139] Q. Cao, S.-H. Hur, Z.-T. Zhu, Y. G. Sun, C.-J. Wang, M. A. Meitl, M. Shim, J. A. Rogers, *Adv. Mater.* **2006**, *18*, 304.
[140] Y.-L. Rao, A. Chortos, R. Pfattner, F. Lissel, Y.-C. Chiu, V. Feig, J. Xu, T. Kurosawa, X. Gu, C. Wang, M. He, J. W. Chung, Z. Bao, *J. Am. Chem. Soc.* **2016**, *138*, 6020.
[141] D. Kong, R. Pfattner, A. Chortos, C. Lu, A. C. Hinckley, C. Wang, W.-Y. Lee, J. W. Chung, Z. Bao, *Adv. Funct. Mater.* **2016**, *26*, 4680.
[142] L. Cai, S. Zhang, J. Miao, Z. Yu, C. Wang, *ACS Nano* **2016**, *10*, 11459.
[143] C. Huang, Q. M. Zhang, G. deBotton, K. Bhattacharya, *Appl. Phys. Lett.* **2004**, *84*, 4391.
[144] B. Kang, E. Song, S. B. Lee, B.-G. Chae, H. Ahn, K. Cho, *Chem. Mater.* **2018**, *30*, 6353.
[145] W. Hu, S. N. Zhang, X. Niu, C. Liu, Q. Pei, *J. Mater. Chem. C* **2014**, *2*, 1658.
[146] A. Bele, C. Tugui, L. Sacarescu, M. Iacob, G. Stiubianu, M. Dascalu, C. Racles, M. Cazacu, *Mater. Des.* **2018**, *141*, 120.
[147] A. Chortos, G. I. Koleilat, R. Pfattner, D. Kong, P. Lin, R. Nur, T. Lei, H. Wang, N. Liu, Y.-C. Lai, M.-G. Kim, J. W. Chung, S. Lee, Z. Bao, *Adv. Mater.* **2016**, *28*, 4441.
[148] A. Chortos, C. Zhu, J. Y. Oh, X. Yan, I. Pochorovski, J. W. F. To, N. Liu, U. Kraft, B. Murmann, Z. Bao, *ACS Nano* **2017**, *11*, 7925.
[149] C. Ma, Y. Gong, R. Lu, E. Brown, B. Ma, J. Li, J. Wu, *Nanoscale* **2015**, *7*, 18489.
[150] E. Orgiu, S. Locci, B. Fraboni, E. Scavetta, P. Lugli, A. Bonfiglio, *Org. Electron.* **2011**, *12*, 477.
[151] C. Lu, W.-Y. Lee, C.-C. Shih, M.-Y. Wen, W.-C. Chen, *ACS Appl. Mater. Interfaces* **2017**, *9*, 25522.
[152] J. Le Bideau, L. Viau, A. Vioux, *Chem. Soc. Rev.* **2011**, *40*, 907.
[153] M. C. Buzzeo, R. G. Evans, R. G. Compton, *ChemPhysChem* **2004**, *5*, 1106.
[154] T. Ueki, M. Watanabe, *Macromolecules* **2008**, *41*, 3739.
[155] J. H. Cho, J. Lee, Y. He, B. S. Kim, T. P. Lodge, C. D. Frisbie, *Adv. Mater.* **2008**, *20*, 686.
[156] J. Lee, M. J. Panzer, Y. He, T. P. Lodge, C. D. Frisbie, *J. Am. Chem. Soc.* **2007**, *129*, 4532.
[157] K. Melzer, M. Brändlein, B. Popescu, D. Popescu, P. Lugli, G. Scarpa, *Faraday Discuss.* **2014**, *174*, 399.
[158] H. M. Yang, Y. K. Kwon, S. B. Lee, S. Kim, K. Hong, K. H. Lee, *ACS Appl. Mater. Interfaces* **2017**, *9*, 8813.
[159] E. M. Jung, S. W. Lee, S. H. Kim, *Org. Electron.* **2018**, *52*, 123.
[160] C. Leighton, *Nat. Mater.* **2019**, *18*, 13.
[161] Y. Ren, H. Yuan, X. Wu, Z. Chen, Y. Iwasa, Y. Cui, H. Y. Hwang, K. Lai, *Nano Lett.* **2015**, *15*, 4730.
[162] M. S. Barbosa, F. M. B. Oliveira, X. Meng, F. Soavi, C. Santato, M. O. Orlandi, *J. Mater. Chem. C* **2018**, *6*, 1980.
[163] K. H. Seol, S. J. Lee, K. G. Cho, K. Hong, K. H. Lee, *J. Mater. Chem. C* **2018**, *6*, 10987.
[164] G. D. Spyropoulos, J. N. Gelinas, D. Khodagholy, *Sci. Adv.* **2019**, *5*, eaau7378.
[165] J. Xu, J. Jia, S. Lai, J. Ju, S. Lee, *Appl. Phys. Lett.* **2017**, *110*, 033103.
[166] S.-K. Lee, B. J. Kim, H. Jang, S. C. Yoon, C. Lee, B. H. Hong, J. A. Rogers, J. H. Cho, J.-H. Ahn, *Nano Lett.* **2011**, *11*, 4642.
[167] J. Pu, Y. Zhang, Y. Wada, J. T.-W. Wang, L.-J. Li, Y. Iwasa, T. Takenobu, *Appl. Phys. Lett.* **2013**, *103*, 023505.
[168] F. Xu, M.-Y. Wu, N. S. Safron, S. S. Roy, R. M. Jacobberger, D. J. Bindl, J.-H. Seo, T.-H. Chang, Z. Ma, M. S. Arnold, *Nano Lett.* **2014**, *14*, 682.
[169] C. Zhu, A. Chortos, Y. Wang, R. Pfattner, T. Lei, A. C. Hinckley, I. Pochorovski, X. Yan, J. W. F. To, J. Y. Oh, J. B. H. Tok, Z. Bao, B. Murmann, *Nat. Electron.* **2018**, *1*, 183.
[170] C. Larson, B. Peele, S. Li, S. Robinson, M. Totaro, L. Beccai, B. Mazzolai, R. Shepherd, *Science* **2016**, *351*, 1071.
[171] J. Wang, C. Yan, K. J. Chee, P. S. Lee, *Adv. Mater.* **2015**, *27*, 2876.
[172] J. Wang, C. Yan, G. Cai, M. Cui, A. Lee-Sie Eh, P. See Lee, *Adv. Mater.* **2016**, *28*, 4490.
[173] C. H. Yang, B. Chen, J. Zhou, Y. M. Chen, Z. Suo, *Adv. Mater.* **2016**, *28*, 4480.
[174] Z. Yu, X. Niu, Z. Liu, Q. Pei, *Adv. Mater.* **2011**, *23*, 3989.
[175] S. Jung, J. H. Kim, J. Kim, S. Choi, J. Lee, I. Park, T. Hyeon, D.-H. Kim, *Adv. Mater.* **2014**, *26*, 4825.
[176] H. Qin, R. E. Owyeung, S. R. Sonkusale, M. J. Panzer, *J. Mater. Chem. C* **2019**, *7*, 601.
[177] C. M. Boutry, Y. Kaizawa, B. C. Schroeder, A. Chortos, A. Legrand, Z. Wang, J. Chang, P. Fox, Z. Bao, *Nat. Electron.* **2018**, *1*, 314.
[178] C.-L. Choong, M.-B. Shim, B.-S. Lee, S. Jeon, D.-S. Ko, T.-H. Kang, J. Bae, S. H. Lee, K.-E. Byun, J. Im, Y. J. Jeong, C. E. Park, J.-J. Park, U.-I. Chung, *Adv. Mater.* **2014**, *26*, 3451.

[179] H.-H. Chou, A. Nguyen, A. Chortos, J. W. F. To, C. Lu, J. Mei, T. Kurosawa, W.-G. Bae, J. B. H. Tok, Z. Bao, *Nat. Commun.* **2015**, *6*, 8011.
[180] D. J. Lipomi, M. Vosgueritchian, B. C. K. Tee, S. L. Hellstrom, J. A. Lee, C. H. Fox, Z. Bao, *Nat. Nanotechnol.* **2011**, *6*, 788.
[181] Y.-L. Park, C. Majidi, R. Kramer, P. Bérard, R. J. Wood, *J. Micromech. Microeng.* **2010**, *20*, 125029.
[182] T. Wang, Y. Zhang, Q. Liu, W. Cheng, X. Wang, L. Pan, B. Xu, H. Xu, *Adv. Funct. Mater.* **2018**, *28*, 1705551.
[183] L. Cai, L. Song, P. Luan, Q. Zhang, N. Zhang, Q. Gao, D. Zhao, X. Zhang, M. Tu, F. Yang, W. Zhou, Q. Fan, J. Luo, W. Zhou, P. M. Ajayan, S. Xie, *Sci. Rep.* **2013**, *3*, 3048.
[184] H. Xu, Y. Lv, D. Qiu, Y. Zhou, H. Zeng, Y. Chu, *Nanoscale* **2019**, *11*, 1570.
[185] N. Lu, C. Lu, S. Yang, J. Rogers, *Adv. Funct. Mater.* **2012**, *22*, 4044.
[186] J. T. Muth, D. M. Vogt, R. L. Truby, Y. Mengüç, D. B. Kolesky, R. J. Wood, J. A. Lewis, *Adv. Mater.* **2014**, *26*, 6307.
[187] J. Shintake, E. Piskarev, S. H. Jeong, D. Floreano, *Adv. Mater. Technol.* **2018**, *3*, 1700284.
[188] T. Q. Trung, S. Ramasundaram, B.-U. Hwang, N.-E. Lee, *Adv. Mater.* **2016**, *28*, 502.
[189] H.-S. Chuang, S. Wereley, *J. Micromech. Microeng.* **2009**, *19*, 045010.
[190] M. L. Jin, S. Park, J.-S. Kim, S. H. Kwon, S. Zhang, M. S. Yoo, S. Jang, H.-J. Koh, S.-Y. Cho, S. Y. Kim, C. W. Ahn, K. Cho, S. G. Lee, D. H. Kim, H.-T. Jung, *Adv. Mater.* **2018**, *30*, 1706851.
[191] T. Q. Trung, L. T. Duy, S. Ramasundaram, N.-E. Lee, *Nano Res.* **2017**, *10*, 2021.
[192] N. Razza, B. Blanchet, A. Lamberti, F. C. Pirri, J.-M. Tulliani, L. D. Bozano, M. Sangermano, *Macromol. Mater. Eng.* **2017**, *302*, 1700161.
[193] S. Wang, J. Xu, W. Wang, G.-J. N. Wang, R. Rastak, F. Molina-Lopez, J. W. Chung, S. Niu, V. R. Feig, J. Lopez, T. Lei, S.-K. Kwon, Y. Kim, A. M. Foudeh, A. Ehrlich, A. Gasperini, Y. Yun, B. Murmann, J. B. H. Tok, Z. Bao, *Nature* **2018**, *555*, 83.
[194] C. Yan, J. Wang, X. Wang, W. Kang, M. Cui, C. Y. Foo, P. S. Lee, *Adv. Mater.* **2014**, *26*, 943.
[195] J. Wang, C. Yan, W. Kang, P. S. Lee, *Nanoscale* **2014**, *6*, 10734.
[196] Y. Li, N. Li, J. Ge, Y. Xue, W. Niu, M. Chen, Y. Du, P. X. Ma, B. Lei, *Biomaterials* **2019**, *201*, 68.